A new global surface current climatology, with application to the Hawaiian Island region

Rick Lumpkin
(Rick.Lumpkin@noaa.gov)

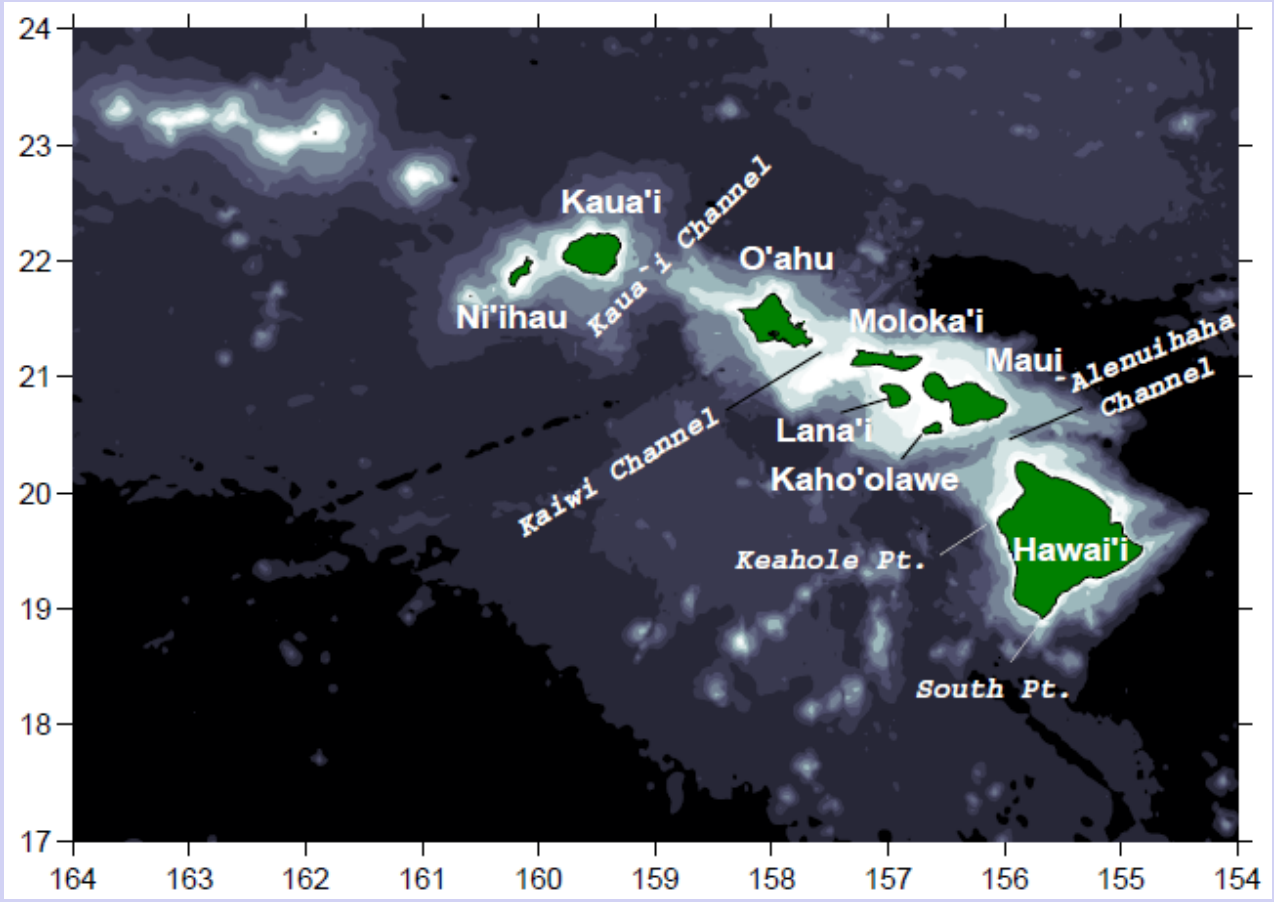

Drogue presence reanalysis

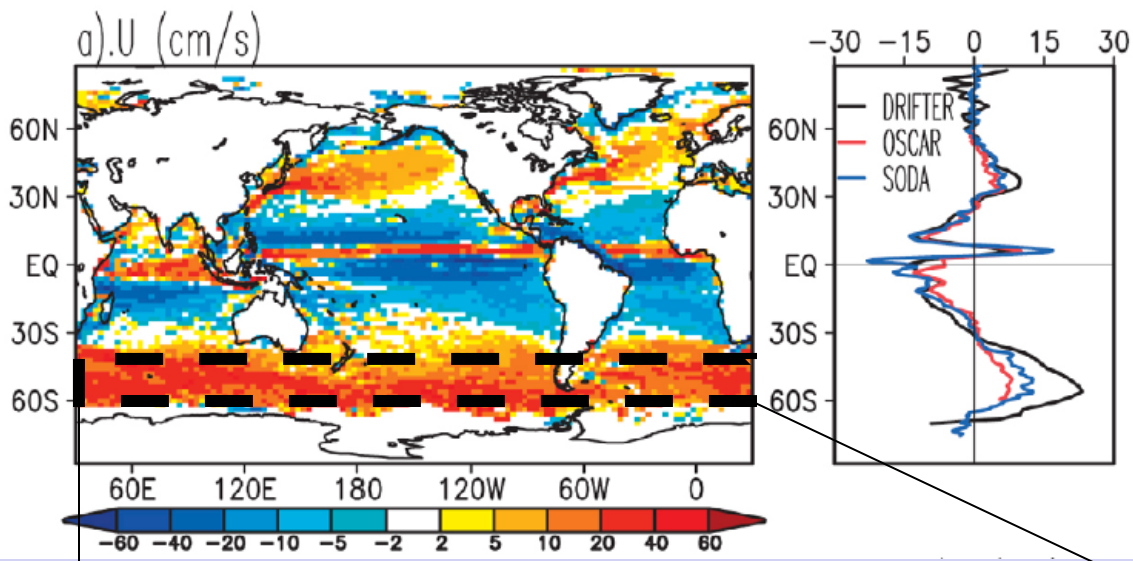

Left: time-mean zonal currents from drifters and two independent analyses (Grodsky *et al*., 2011).

Geostrophic component can be calculated from AVISO and CLS mean dynamic height (Rio *et al*.., 2011).

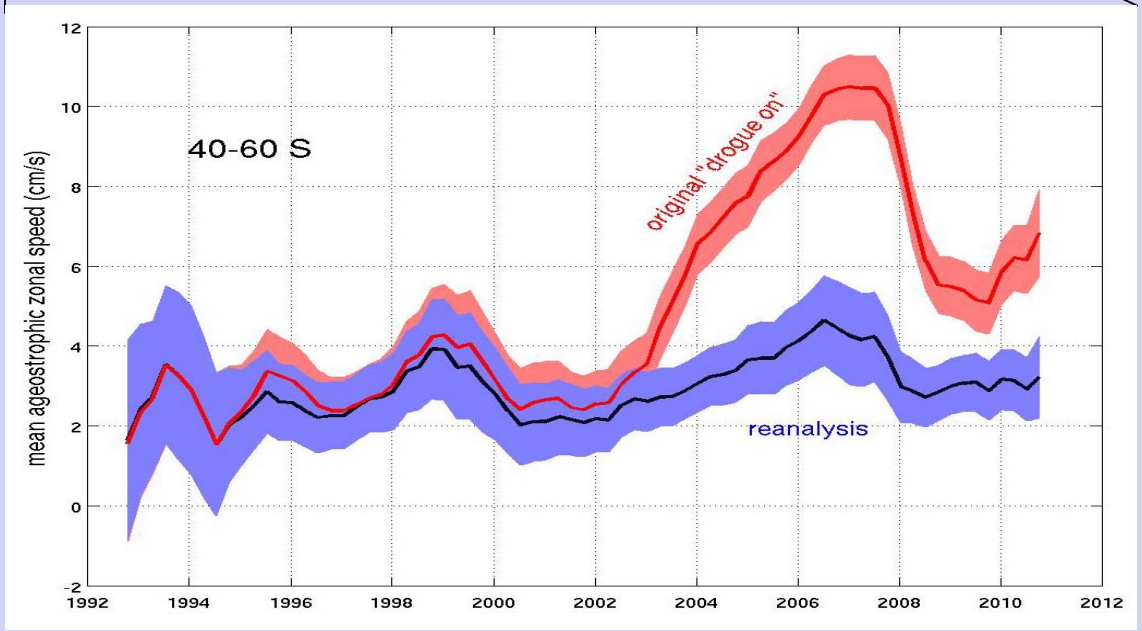

Time mean currents in the ACC band 40—60S before (red) and after (blue) drogue presence reanalysis (Lumpkin et al., 2012).

Observational density

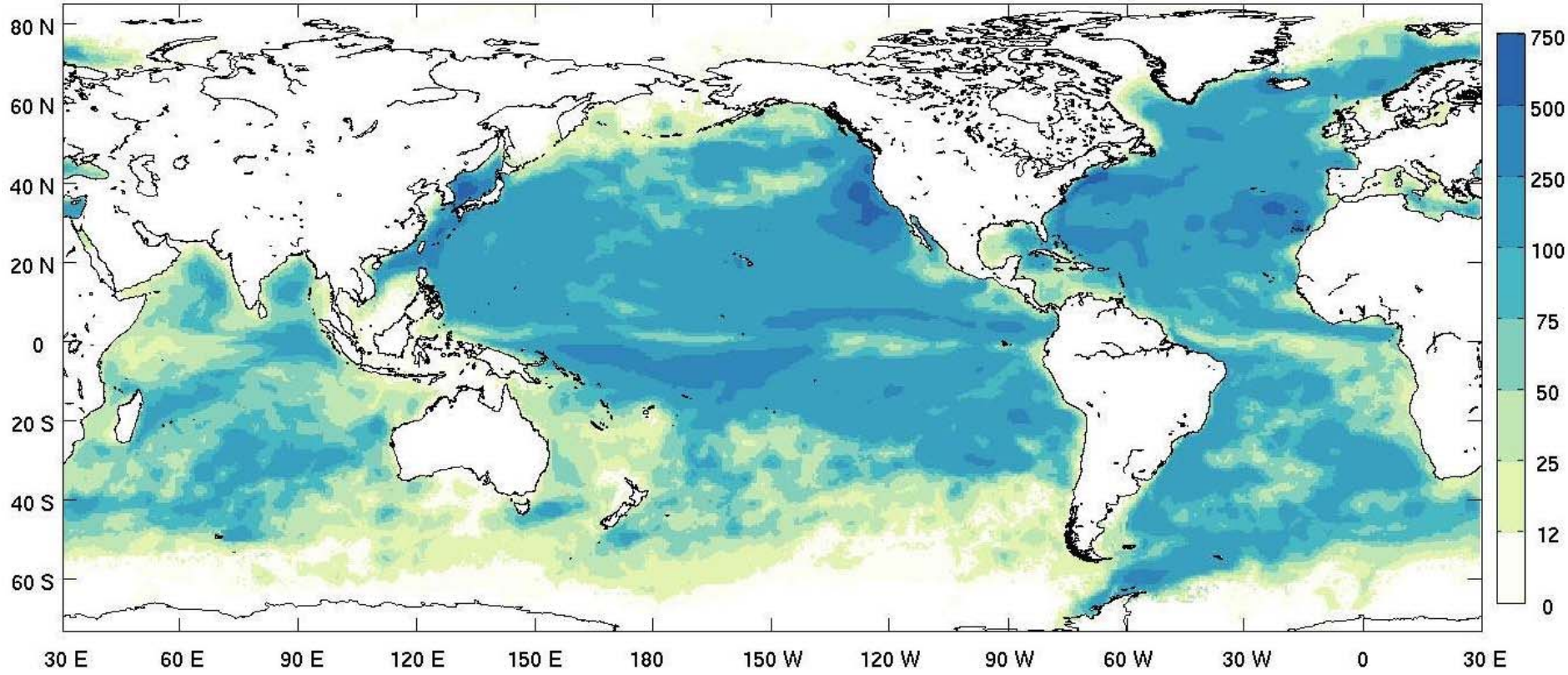

Drogued drifter days per square degree in the bins.
<12: currents not mapped.

Lumpkin and Johnson (2013)

Methodology
(Lumpkin and Johnson, 2013)

- QC, interpolated 6h velocities from drifter DAC.
- Only drogued values (according to recent reanalysis).
- NCEP winds used to remove linear slip.
- Lowpassed at 5 days (remove inertial, tidal).
- Decimated to daily values.

Pseudo-Eulerian means:

- Mapped in elliptical bins of area $\pi \times (1^\circ)^2$.
- Eccentricity, orientation set by variance ellipse in bin.
- Observations in each bin decomposed into time-mean, annual, semiannual, SOI, and spatial gradient components using Gauss-Markov estimation (also yields formal error estimates).

Eddy variations: $u' = \langle u \rangle - u, \quad v' = \langle v \rangle - v$.

Mean currents

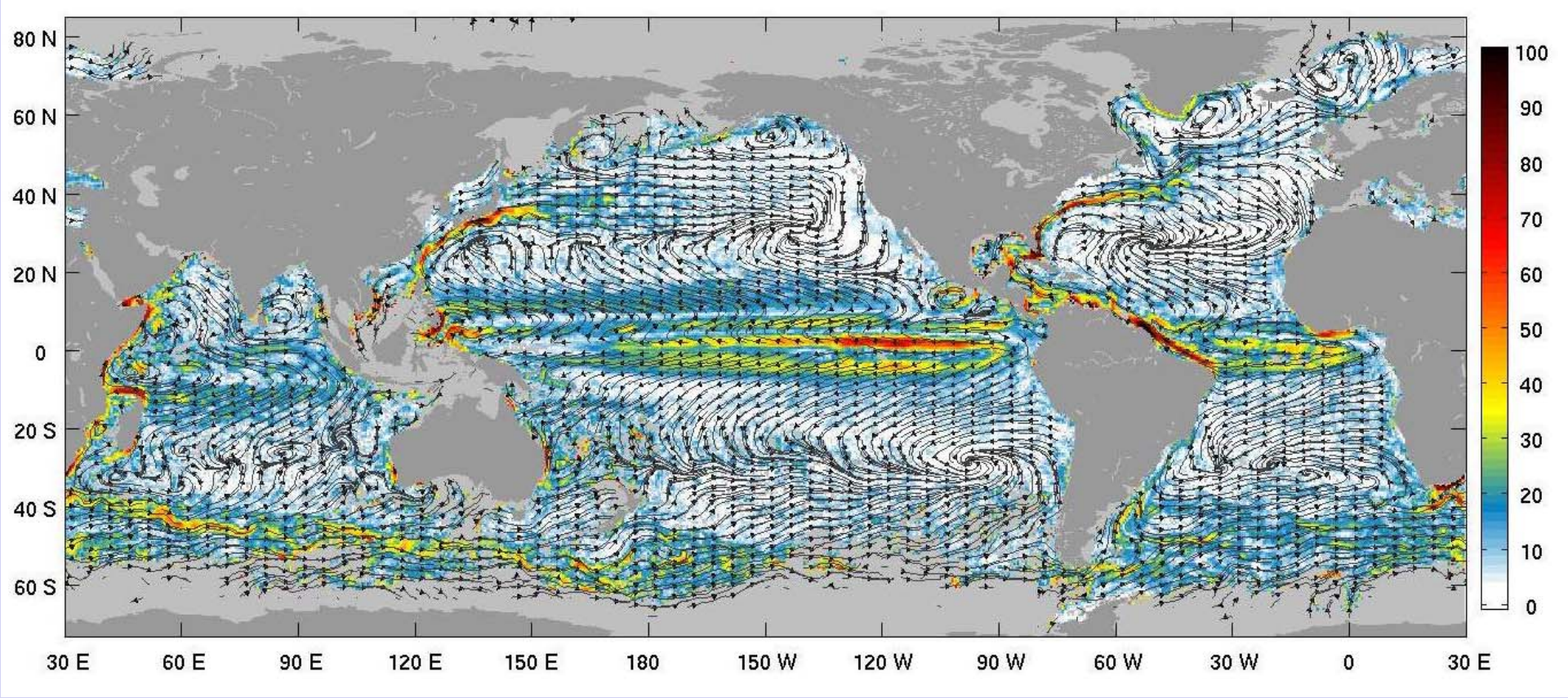

Mean speed (color, in cm s^{-1}) with streamlines (black lines). Gray areas have less than 12 drifter days per square degree. Only bins with mean current speeds statistically different from zero at one standard error of the mean are shaded.

Lumpkin and Johnson (2013)

Residuals (eddies)

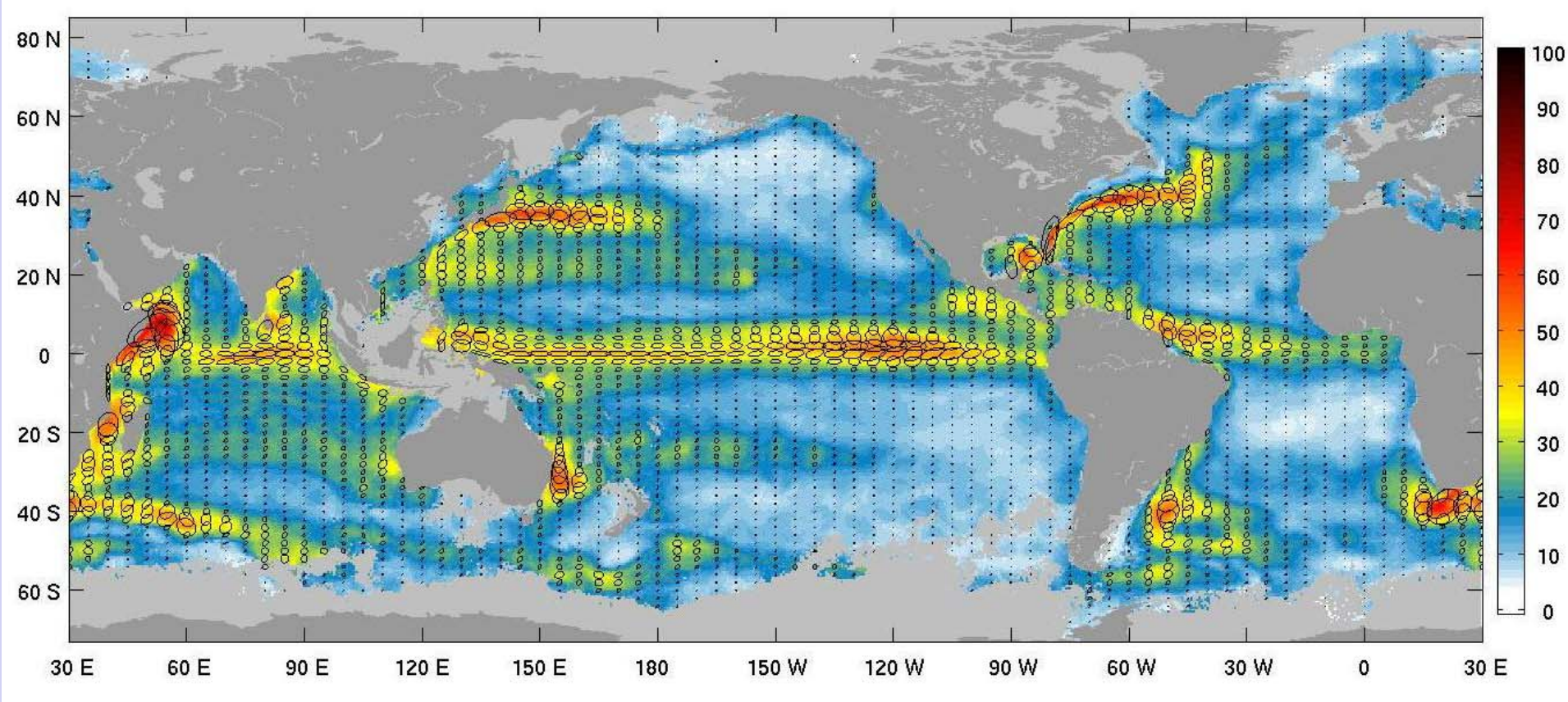

Variance ellipses centered every 5º longitude by 2º latitude. Shading indicates square root of magnitude of variance (cm s^{-1}). Gray areas have less than 12 drifter days per square degree

Lumpkin and Johnson (2013)

Southern Oscillation Index currents

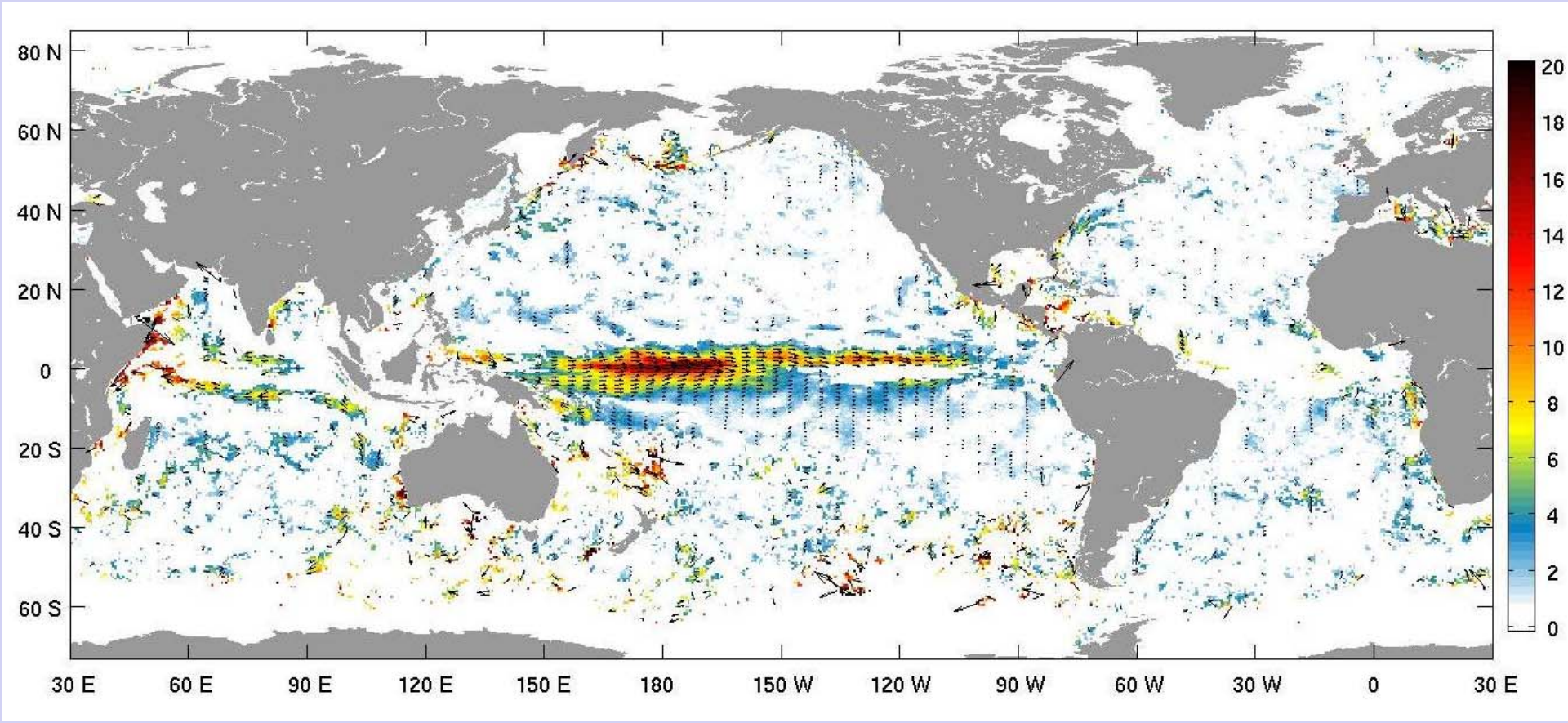

Speed (colors in cm s^{-1}) shown for SOI = -1 (moderate El Niño). Arrows for subset of gridpoints shown to indicate directions. Gridpoints with values not significantly different from zero at one standard error of the mean not displayed

Lumpkin and Johnson (2013)

Islands embedded in large-scale oceanic flow

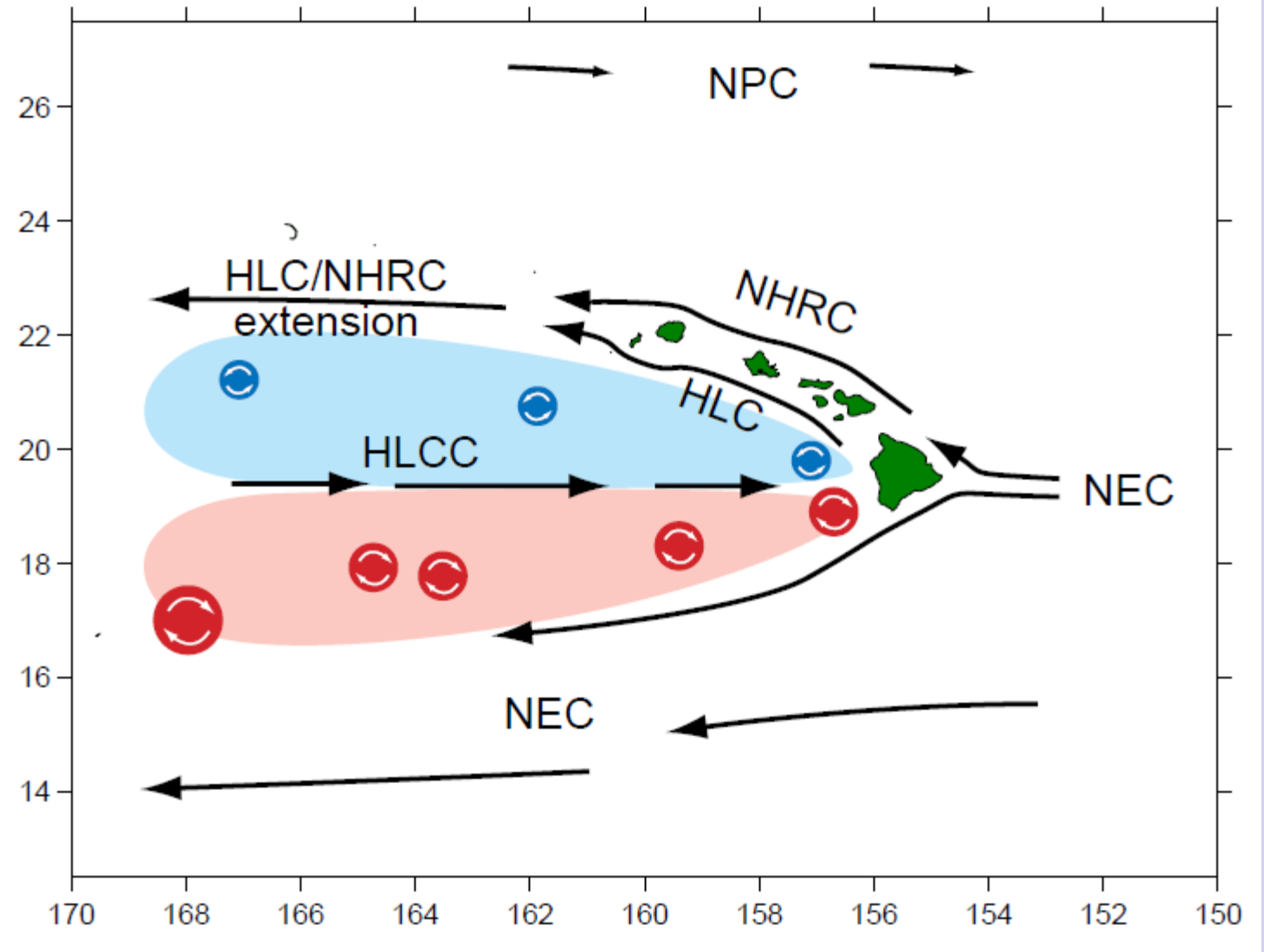

Lumpkin (1998)

Lee eddies

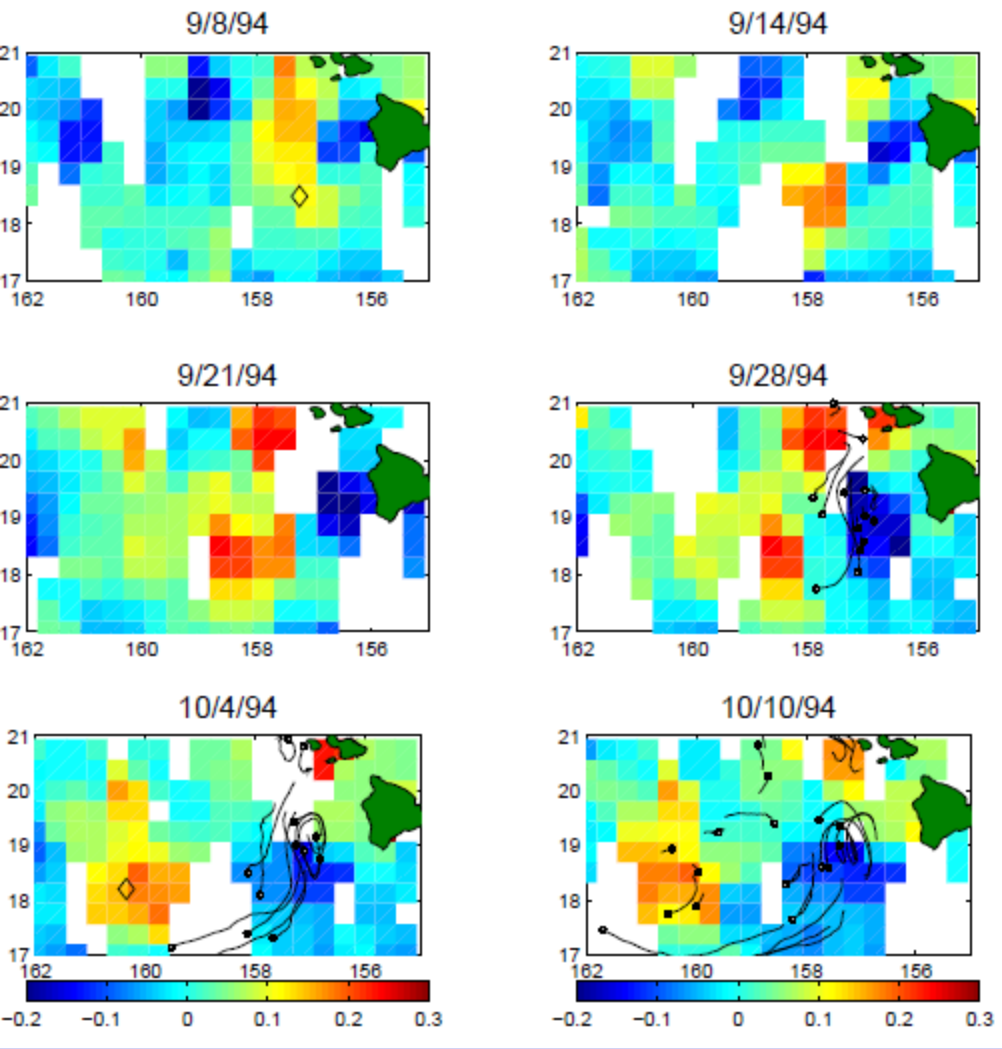

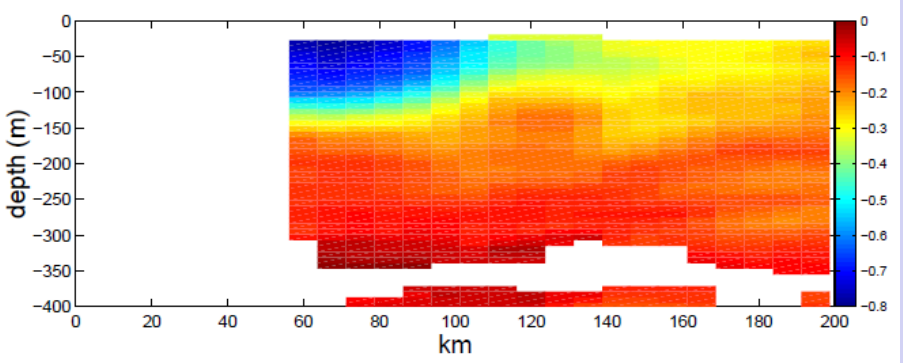

Left: SLA from altimetry, with ADCP-determined center of AC94c (diamonds) and drifter trajectories (black).

Above: ADCP profile of azimuthal speed in AC94c.

Lumpkin (1998)

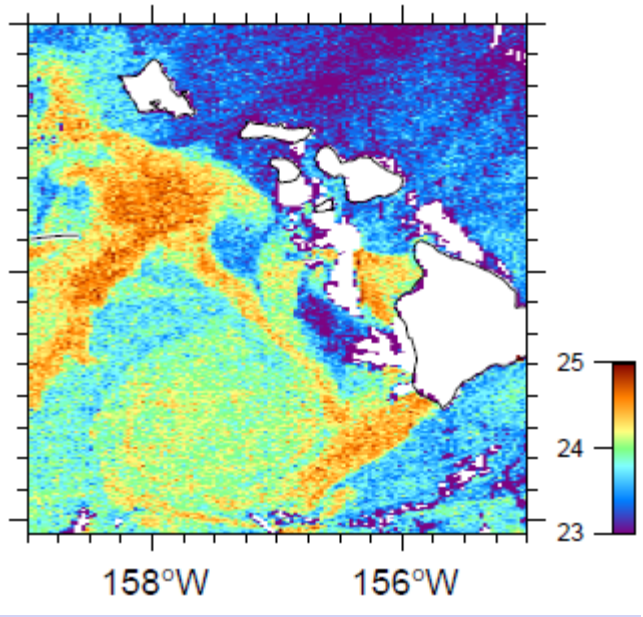

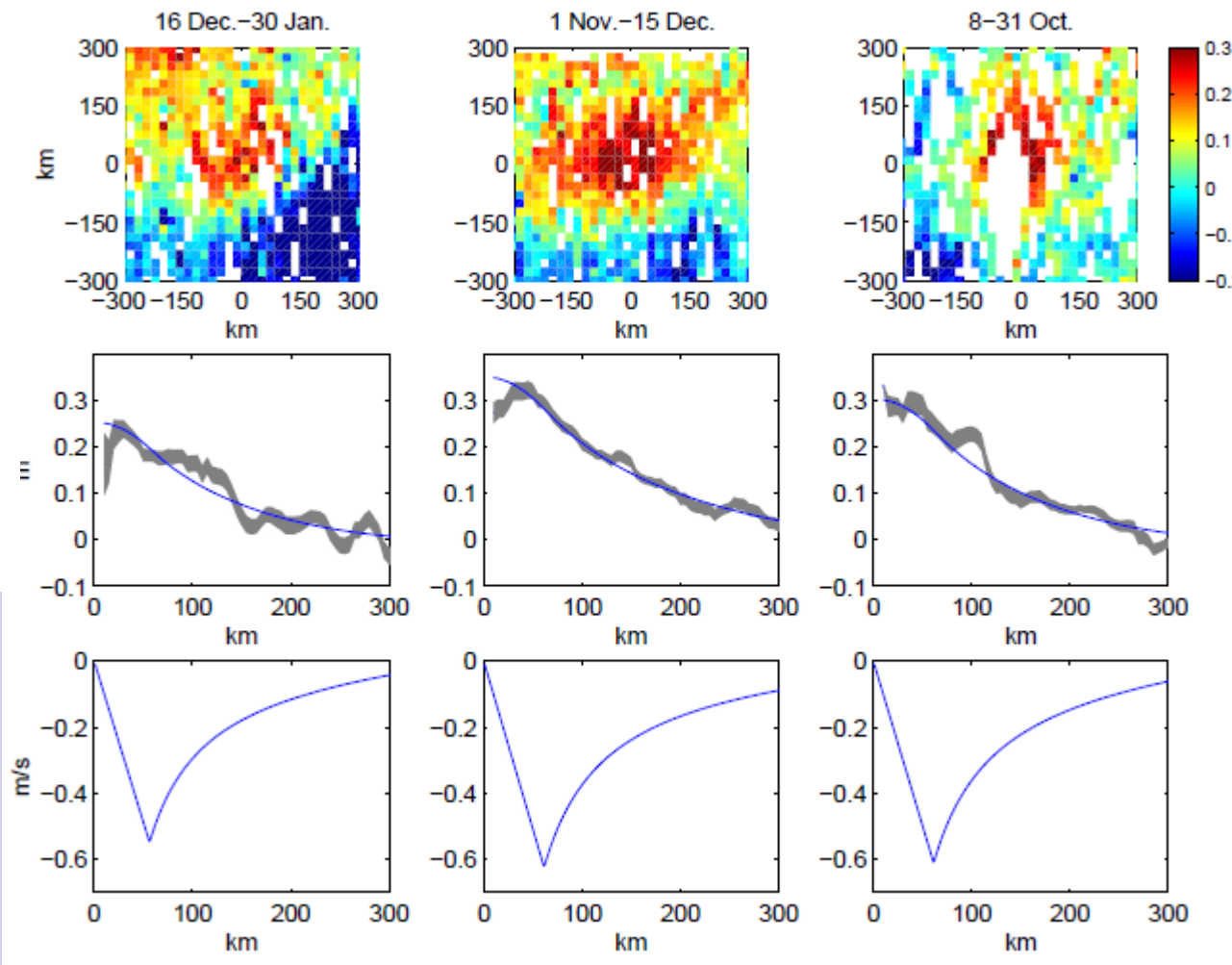

Top: eddy AC94c in AVHRR imagery. **Right**: altimetric passes in frame of reference moving with AC94c.

Lumpkin (1998)

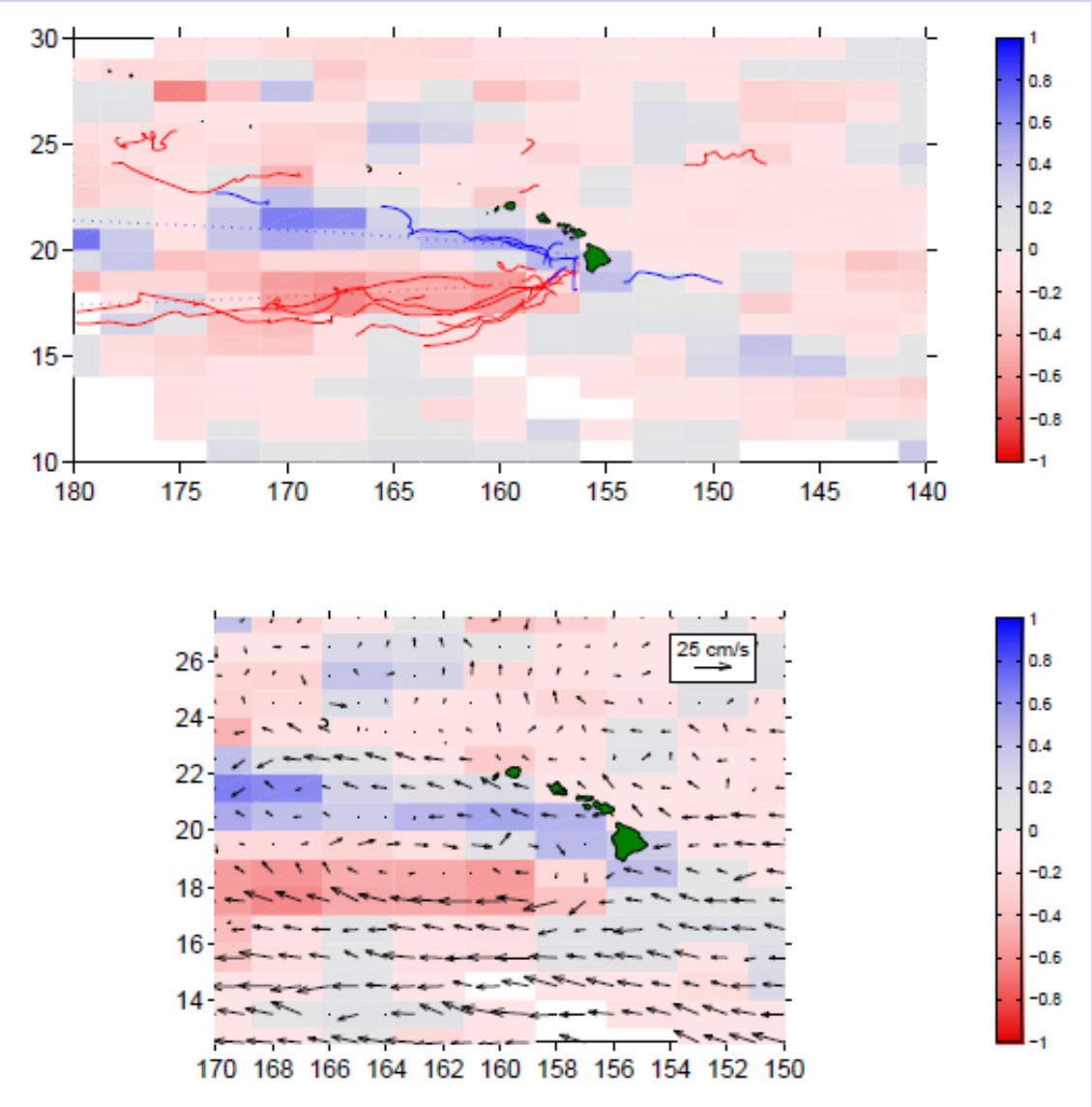

Lumpkin (1998)

Top: mean fraction of subinertial variance into CCW (blue) and CW (red) motion, with paths of cyclonic (blue) and anticyclonic (red) eddies tracked by drifters. **Bottom**: time-mean currents from drifters.

The Hawaiian Lee Countercurrent (HLCC)

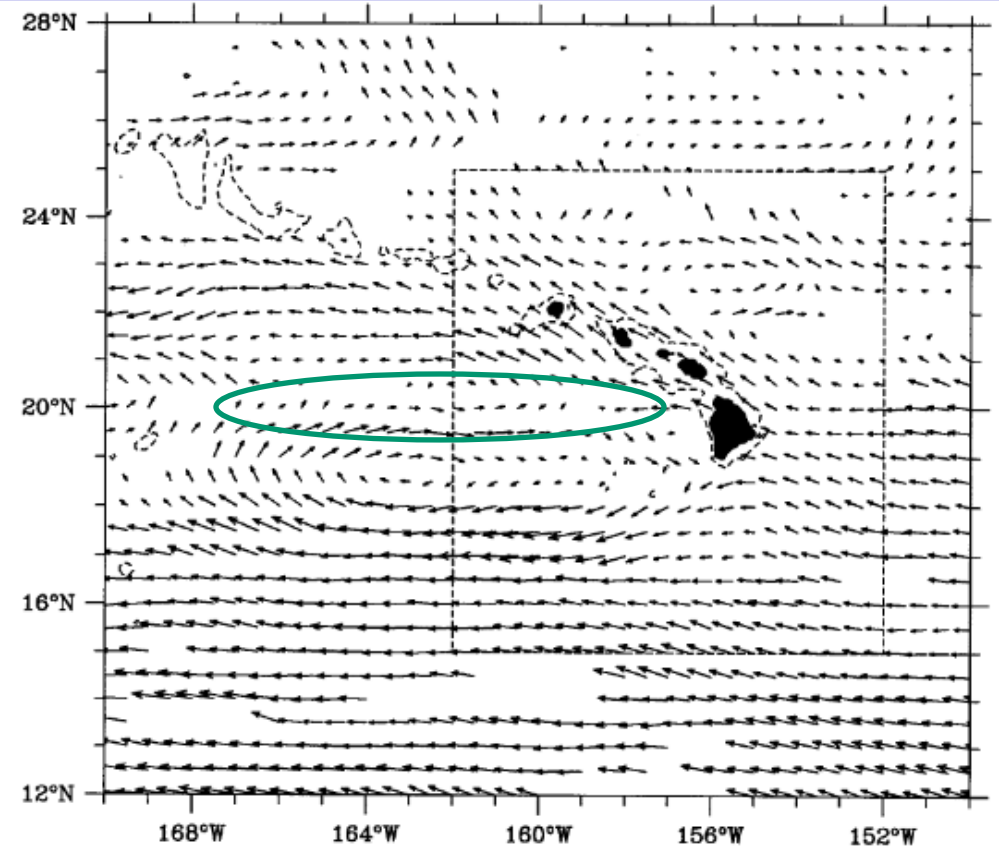

Qiu, Koh, Lumpkin and Flament (1997)

First reported in grey literature from early drifter observations (Flament, 1993, 1994). First documented in peer-reviewed literature by Qiu et al. (1997). Extent: **157—168°W, 19—20°N**.

What is the zonal extent of the HLCC?

Qiu et al. (1997), Lumpkin (1998): **157°W—168°W.**

Drifter data through 1997 → simple bin averaging.

Xie et al. (2001): Hawaiian Islands to Asian coast (!)

1½ layer model, primitive equation model.

Kobashi and Kawamura (2002): "just west of Hawaii" to **150°E.**

CTD, XBT casts → gridded monthly T, S; OI smoothed.

Yu et al. (2003): **158°W—172°W.**

Drifter data through 1999 → simple bin averaging.

158°W—175°W.

2½ layer model. BC instability limits western extent.

Noted that zonal extent very sensitive to model resolution.

Does the barotropic energy flux play a significant role in the HLCC?

Lumpkin (1998): eddy-to-mean flux of 10 ± 8 $\mu W\ m^{-3}$ at 18—19°N, averaged in the band 160—168°W.

Drifter data through 1997.

Yu et al. (2003): no significant BT energy flux averaged in the band 157—172°W.

Drifter data through 1999.

Note: both studies suffered from relatively sparse data dominated by a few dense deployments. Both used simple bin averaging to separate mean/eddy velocities; this can result in biased results (Bauer et al., 1998).

Since 1999: many more drifter observations!

Drogued observations vs. time, 14—25°N, 180—150°W

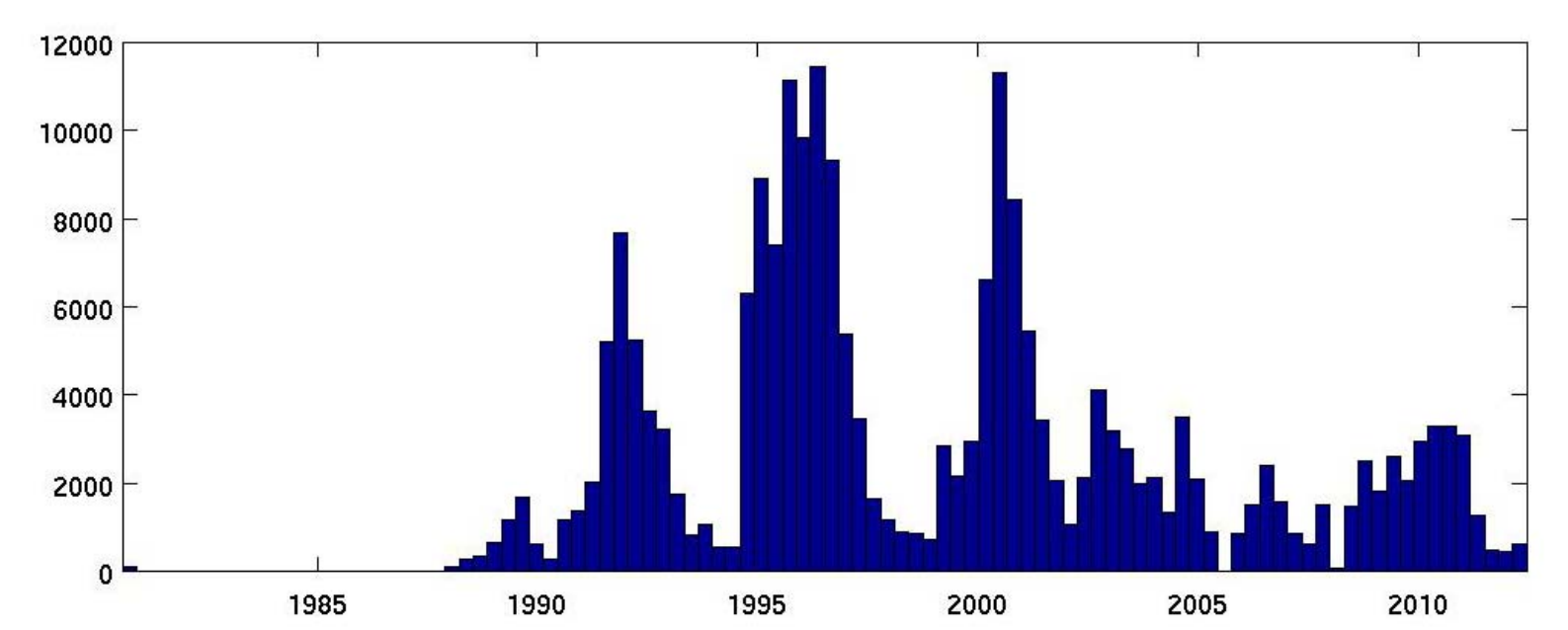

130 drifter-years of drogued velocity data by 324 unique drifters (~ 2× data available through 1999: 64 drifter-years collected by 144 unique drifters).

Data no longer primarily from 1993, 1995 and 1996 deployments.

Since 1999: many more drifter observations!

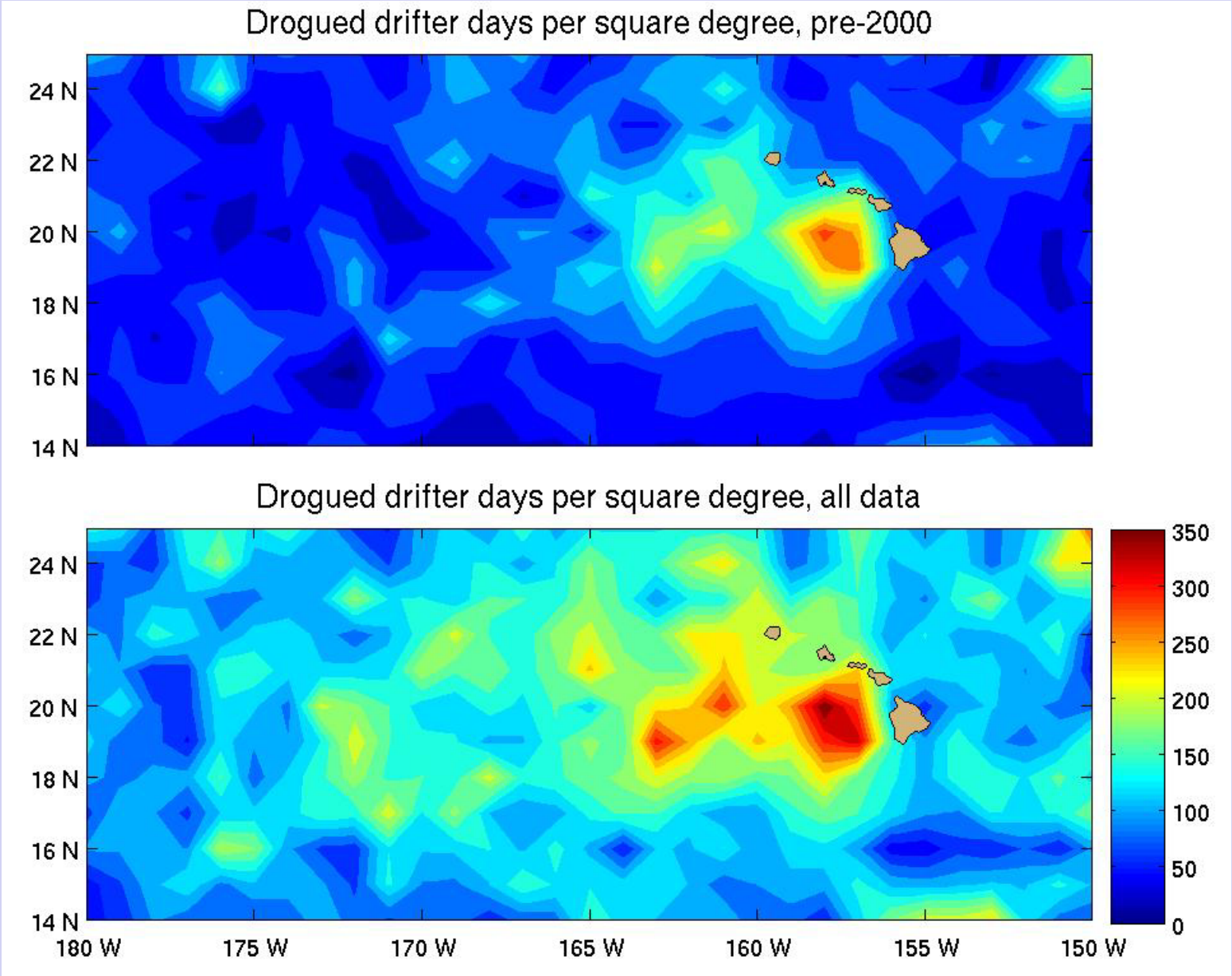

The island wake as seen by drifters

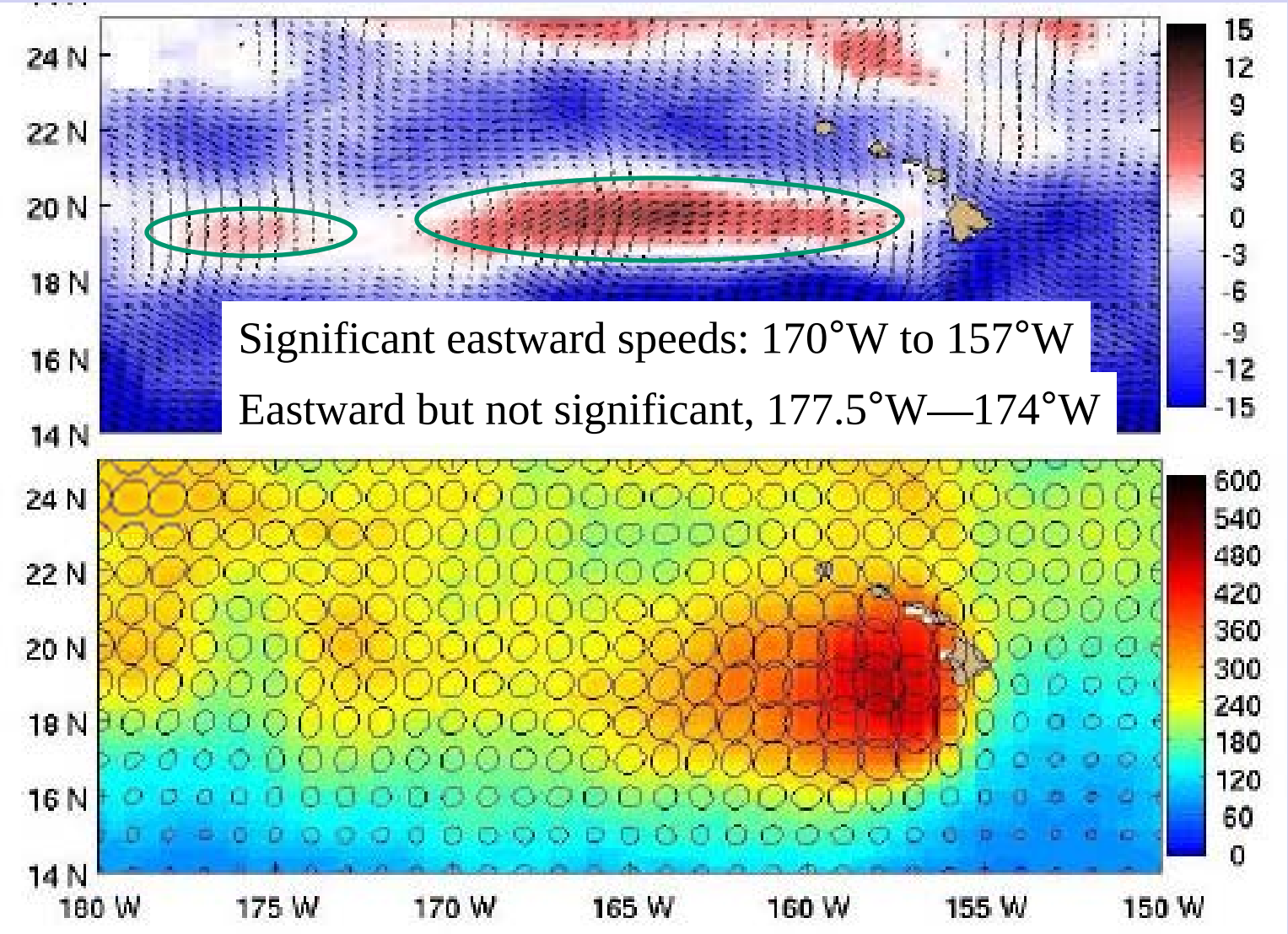

Lumpkin and Flament (2013)

(Animation of seasonal variations in surface currents)

Seasonal variability of the HLCC

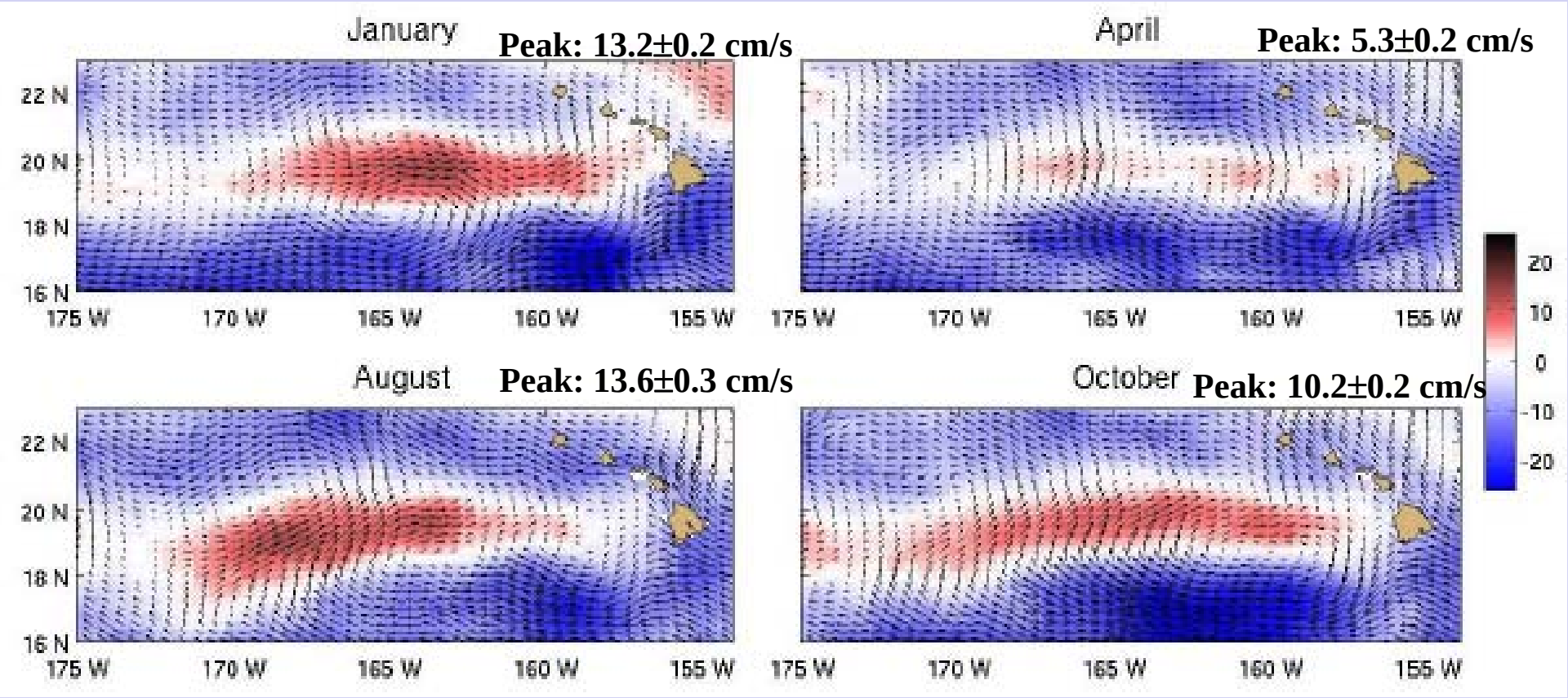

Lumpkin and Flament (2013)

Consistent with Kobashi and Kawamura (2002).

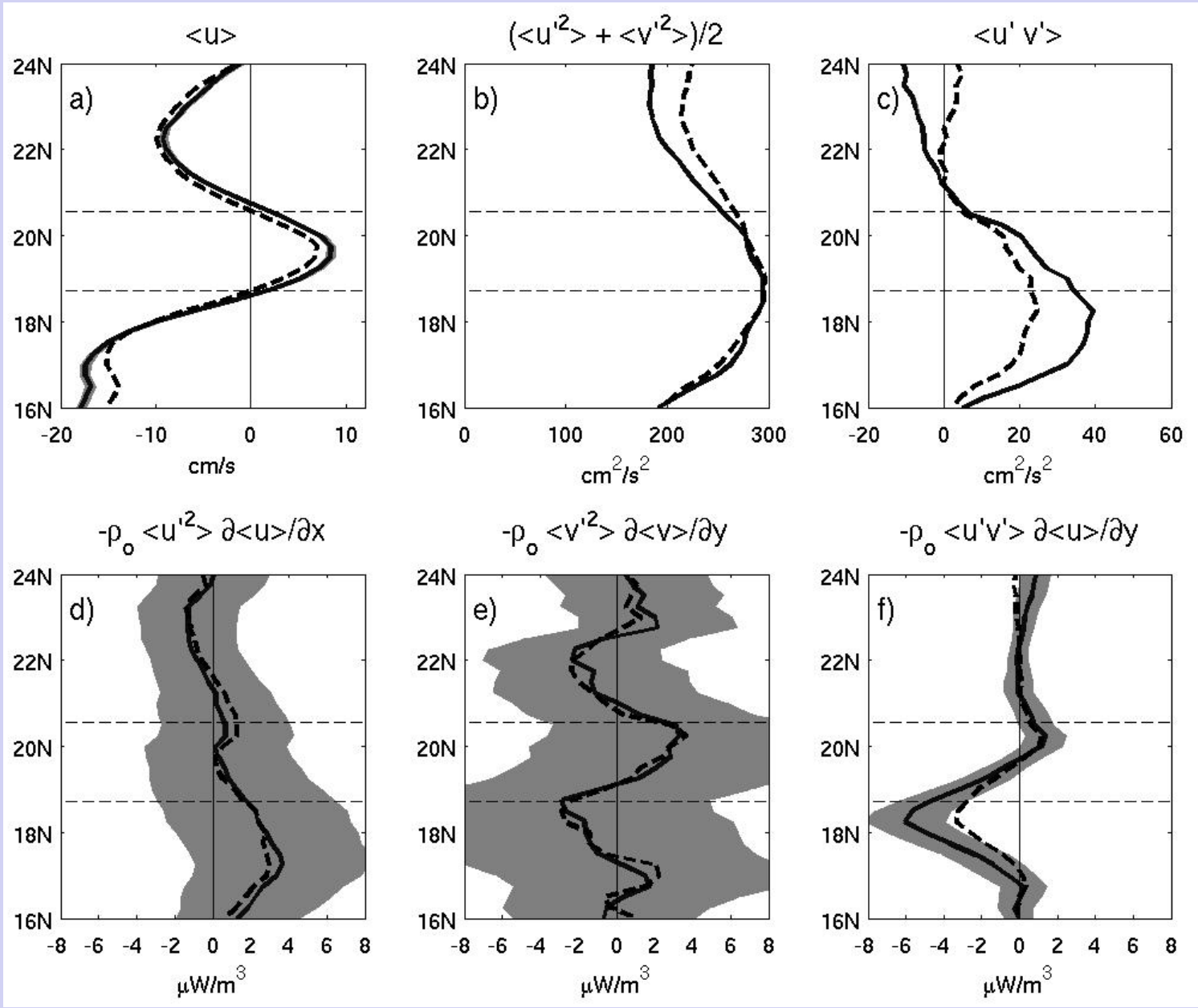

Lumpkin and Flament (2013)

Solid, with error bars: August-January (peak HLCC).
Dashed: annual mean.

The role of the barotropic eddy flux

South of the HLCC, where anticyclonic vorticity dominates the oceanic wake of the Hawaiian Islands, the zonal speed U is strongly meridionally sheared (–10.2 cm s^{-1} at 18.0°N, +6.8 cm s^{-1} at 19.5°N, a mean gradient of 1.0×10^{-6} s^{-1} averaged in the band 160°–168°W)

The Reynolds shear stress $\langle u'v' \rangle$ **works to reinforce this gradient** (25.7±3.0 cm^2 s^{-2} at 18.25°N, 39.5±3.6 cm^2 s^{-2} during peak HLCC months Aug-Jan). The associated eddy-to-mean flux ($\rho \langle u'v' \rangle \partial U/\partial y$) is 3.3±1.2 μW m^{-3} (6.1±2.1 μW m^{-3} during peak months) at 18.25°N. ***Energetic anticyclonic lee eddies advect and deposit zonal momentum that maintains the meridional shear between the HLCC and the NEC to its south.***

This energy flux could spin up an HLCC of U **= 7 cm** s^{-1} **in** time $T = \rho U^2/(2 \times [3$ μW $m^{-3}])$ ~ **10 days, and during peak HLCC months** (U = 8.5 cm s^{-1}) **in seven days**.

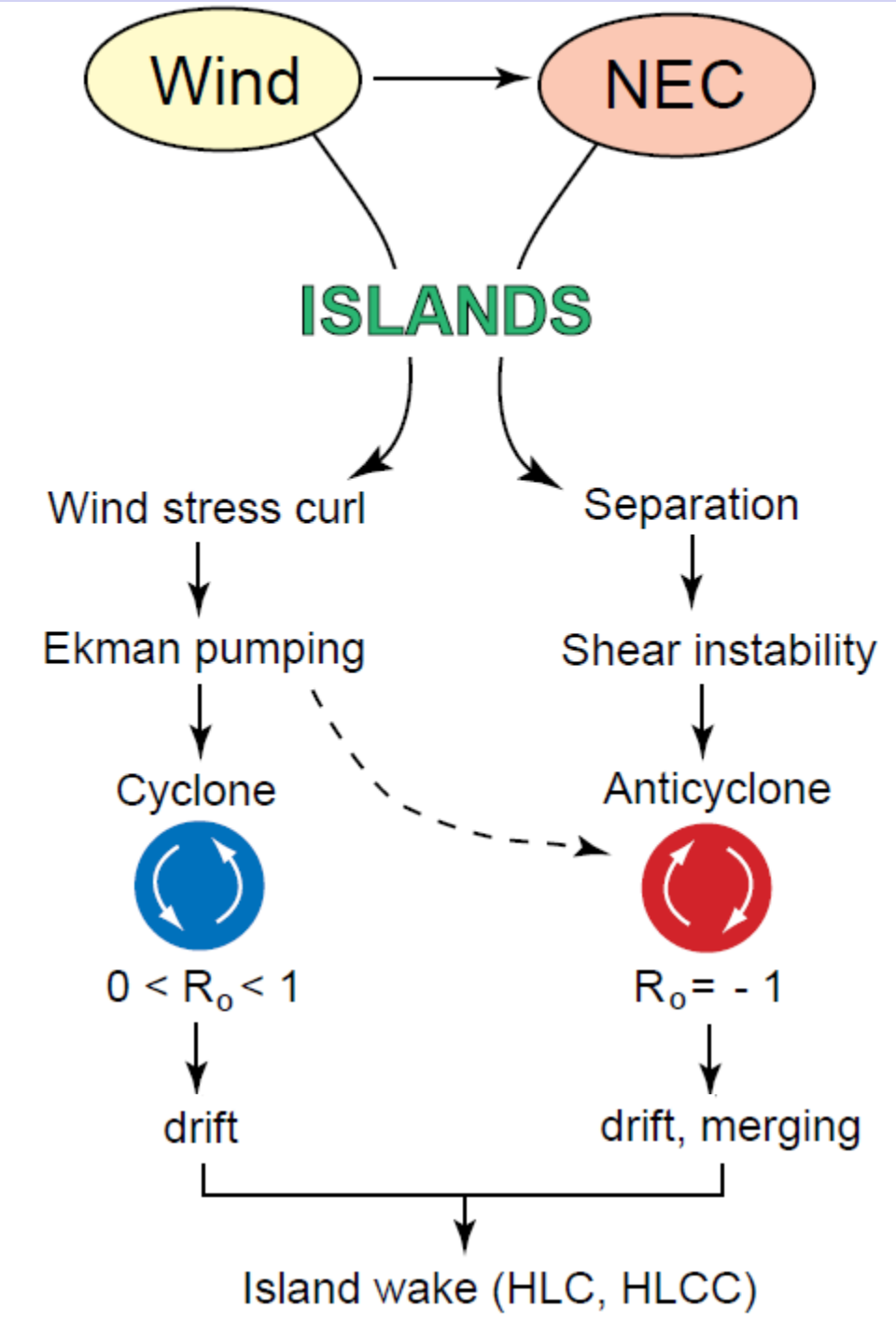

Lumpkin (1998)

Summary

- Drifter observations used to map time-mean, seasonal and SOI-related surface currents.
- Methodology produces formal error bars for all components and for monthly mean fields.
- Study takes advantage of recent drogue reanalysis; only drogued drifters included.
- Results show details of absolute surface circulation at unprecedented resolution.
- Monthly climatology available upon request; to be made publicly available after peer review (manuscript to be submitted to *J. Geophys. Res*.)

Future Work

- Include undrogued drifters using slip correction.
- Separately examine motion that is correlated with local wind (Ekman and slip), and difference (geostrophic).

www.aoml.noaa.gov/phod/dac/dac_meanvel.php

Google YouTube Wikipedia NRT data Weather GDP TropMoorings reference News Misc Guitar Science Blogs ftp on aoml Google mail

The GDP Drifter Data Assembly Center (DAC)

Mean Velocity Estimates

NOAA AOML Physical Oceanography Division

NOAA AOML PhOD Global Ocn Obs GDP **DAC**

Quick Search | Go | Popular topics

Data and Products

Data

- Interpolated Database
- GTS Database
- Altimeter & GTS Near Real Time
- Details of all drifters in DAC database
- ISDM Archives

Products

- Population (Maps and Reports)
- Mean Velocity Estimates
- Animations
- Monthly SST and Current Anomalies Map
- Hurricane Array

Contact

- Contact Information

PhOD project report

Physical Oceanography

A drifter-derived seasonal climatology of global near-surface currents

Version number: 2.05. Created on: 28 August 2013. Most recent data included: 31 December 2012. Documentation: Lumpkin and Johnson (2013). Note: This product reflects results of the recent drogue presence reanalysis (Lumpkin et al., 2013).

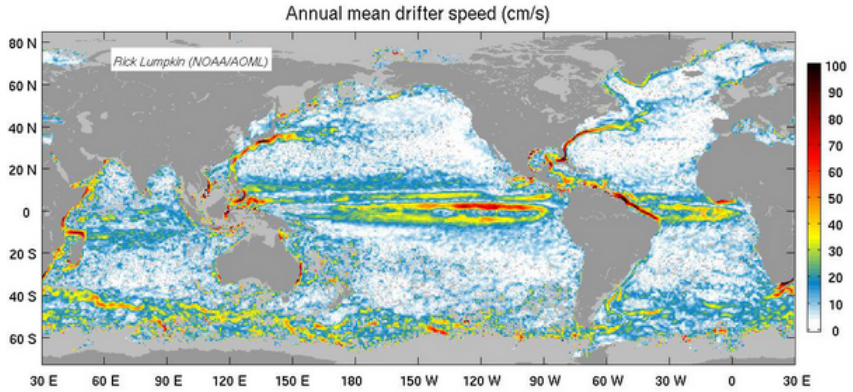

On this page, you will find a seasonal climatology of near-surface currents and SST for the world, at monthly and one-half degree resolution, derived from satellite-tracked surface drifting buoy observations. Animations of these currents are available here. Maps of these currents in various regions can be seen on the Ocean Surface Currents web site.

Climatology available in ASCII, NetCDF and Matlab formats on GDP web page.

Winds around the Hawaiian Islands

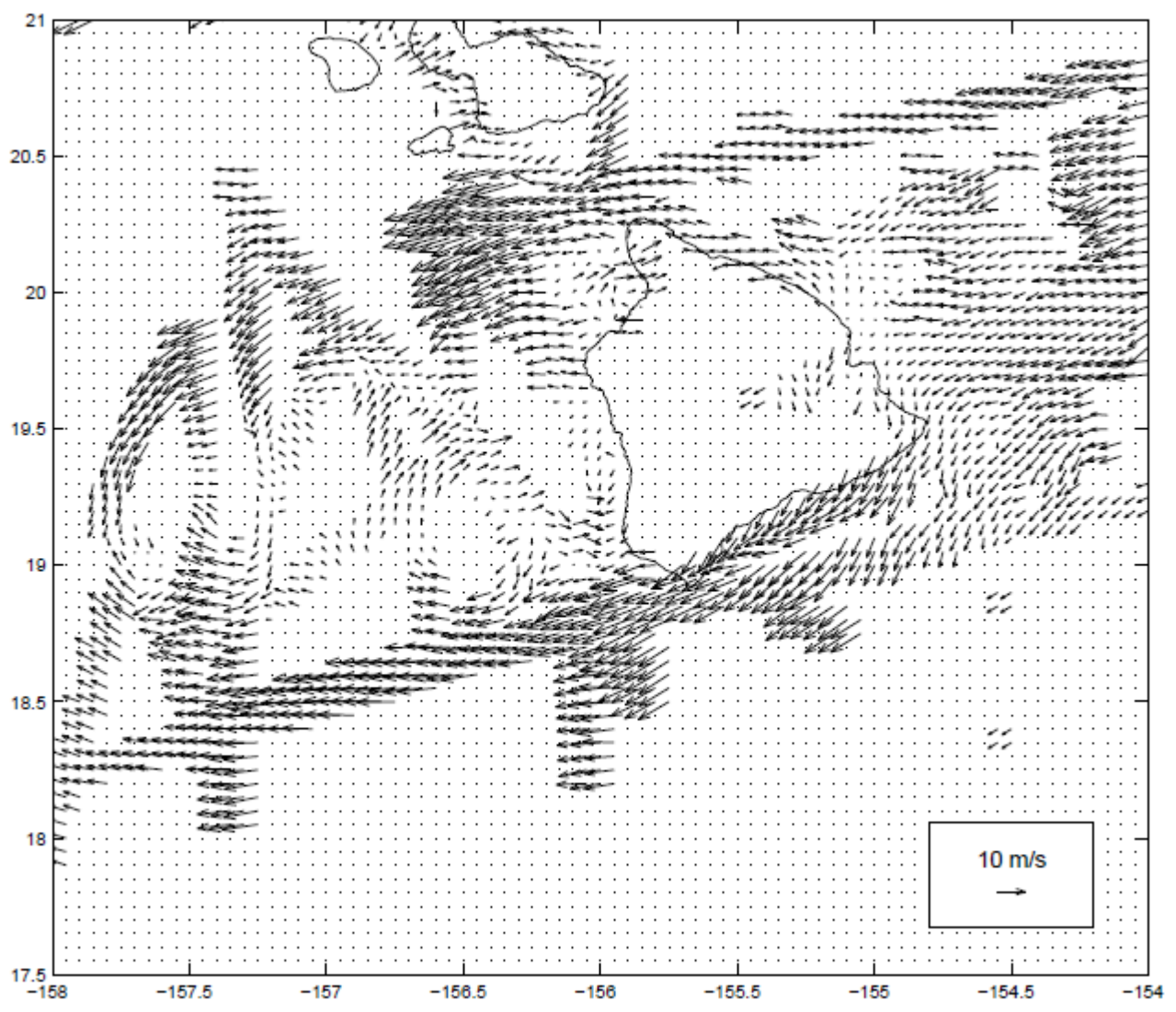

Islands extend above Trade Wind inversion layer.

Wind shadows in island lees.

Wind jets between islands.

Winds at 0-500m measured from the NCAR aircraft Electra during HaRP experiment of July-August 1990 [Smith and Grubisic, 1993; Lumpkin, 1998].

Evidence of large-scale atmospheric wake

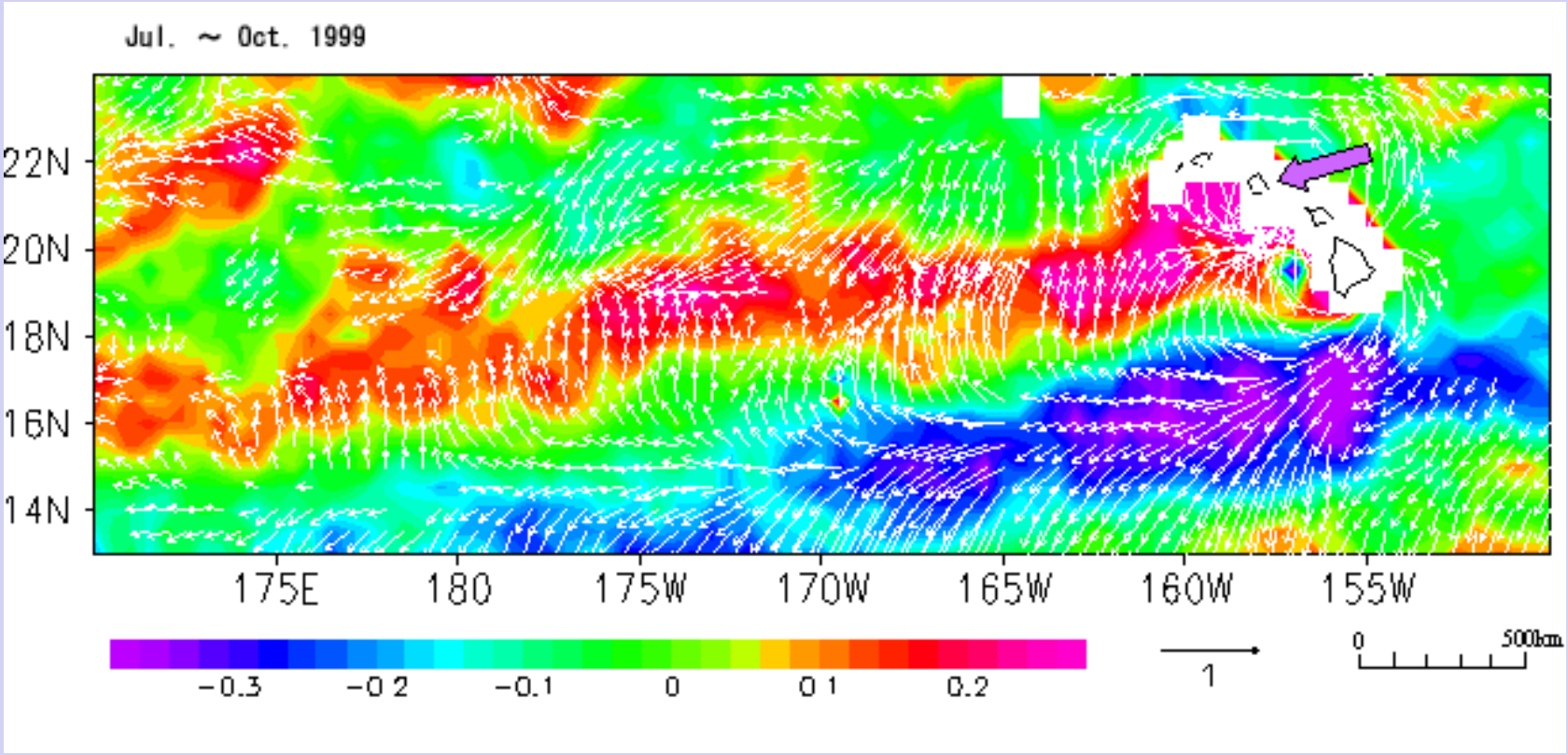

Arrows: QuikSCAT wind stress. Shading: SST anomaly. [from NASA science page “Hawaii’s Wake”].

Evidence of downstream merging

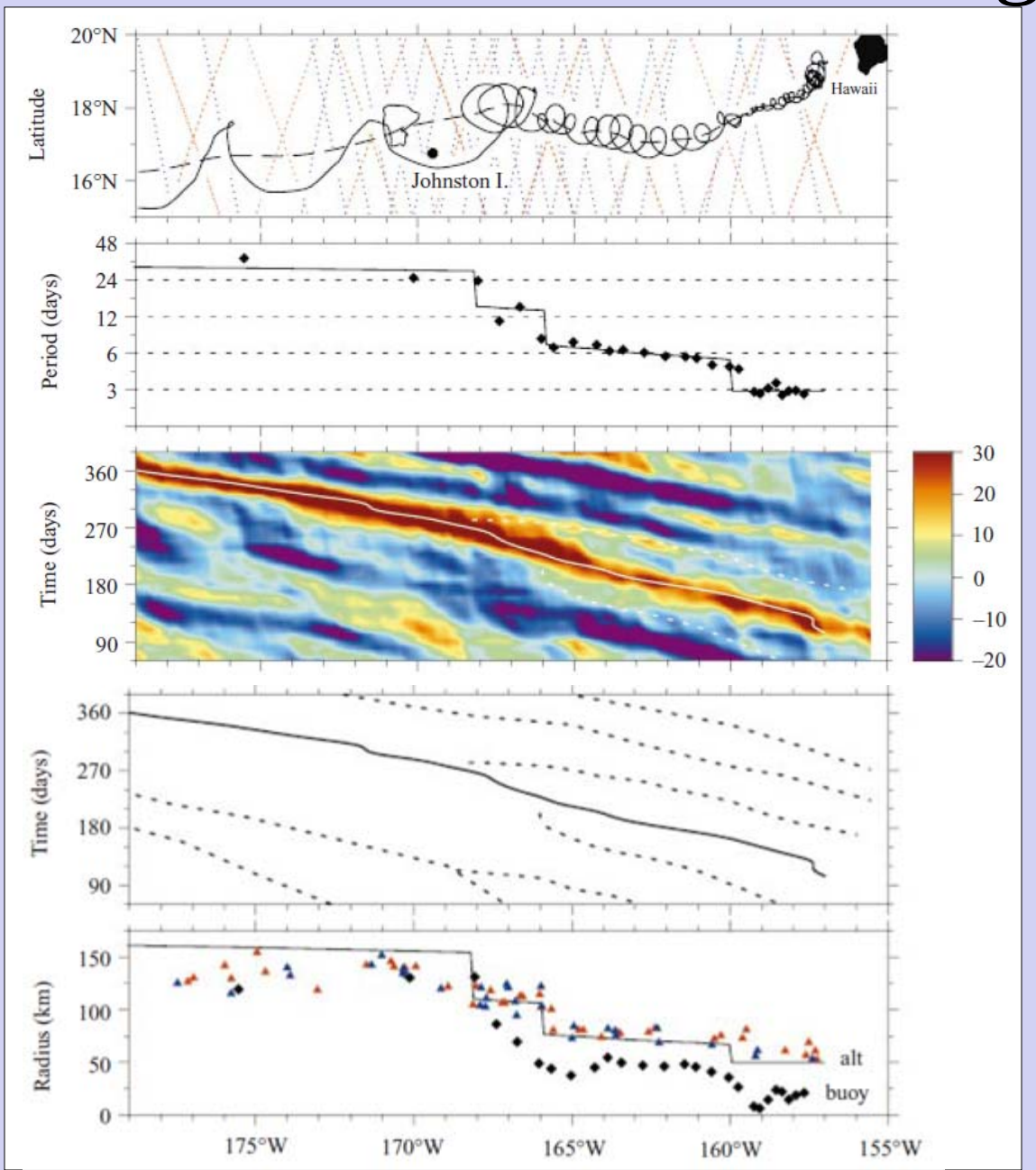

Flament et al. (2001)

What generates the lee eddies?

McGary (1959), Pazert (1968): ***oceanic flow around the Hawaiian Islands*** has Reynolds number in the vortex shedding regime.

Left: atmospheric flow around Guadelupe Island, visualized by clouds, forming Kármán vortex street. Source: http://www.weather.com/news/von-karman-vortices-20130131

Lumpkin (1998): insufficient flow through Alenuihaha Channel. Unstable NEC separation from South Point of Hawaii. Kármán vortex street formation is *stable*.

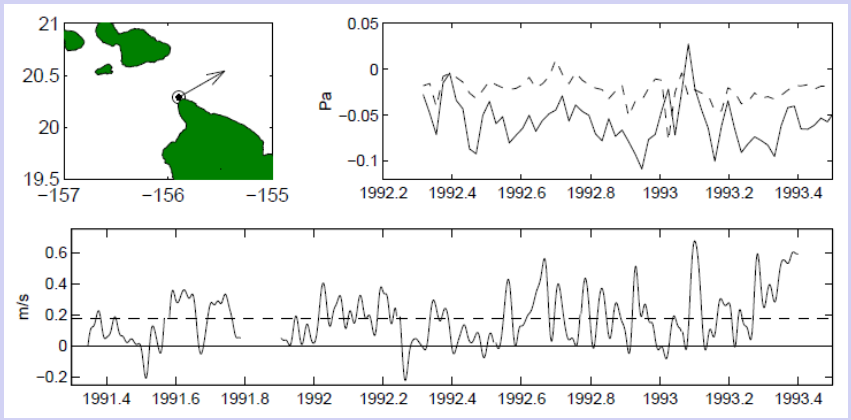

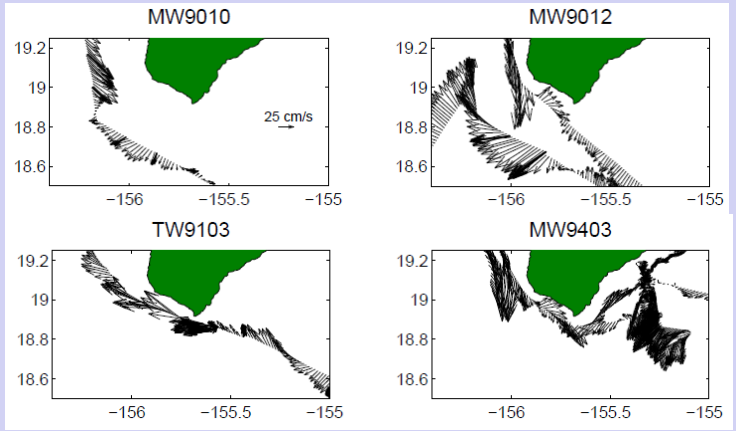

What generates the lee eddies?

Ekman pumping

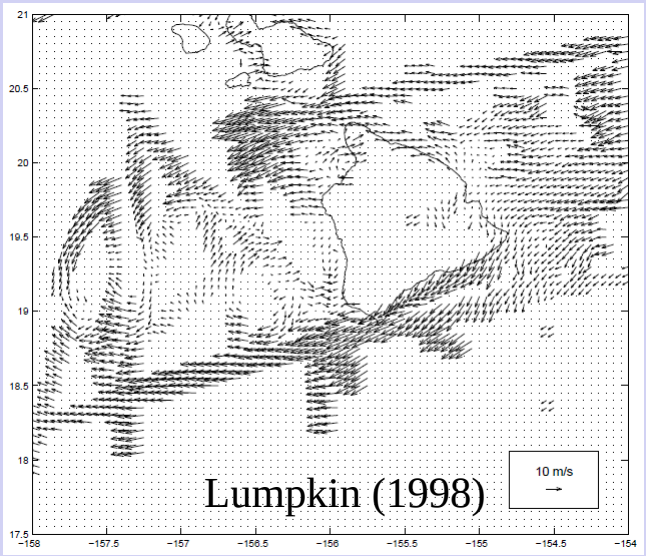

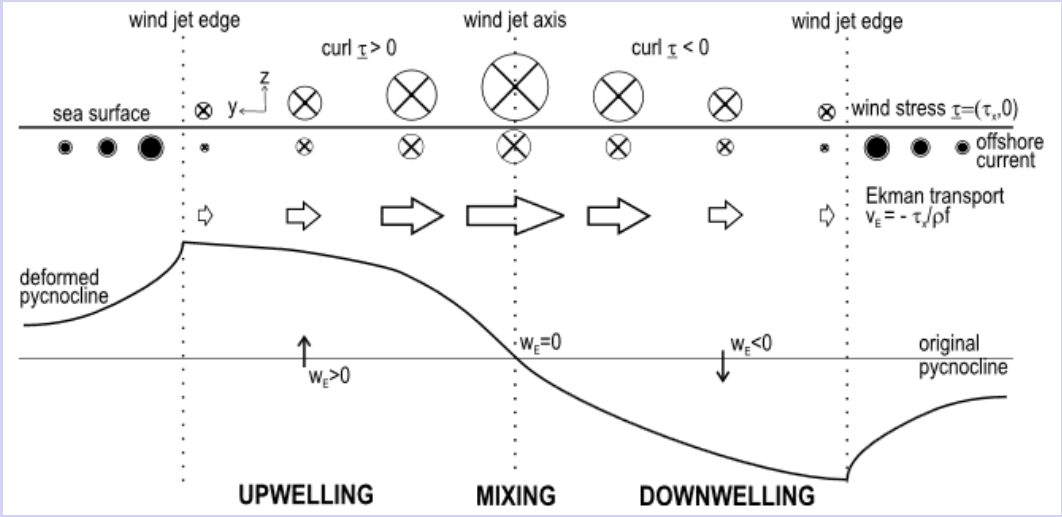

Willett et al. (2006)

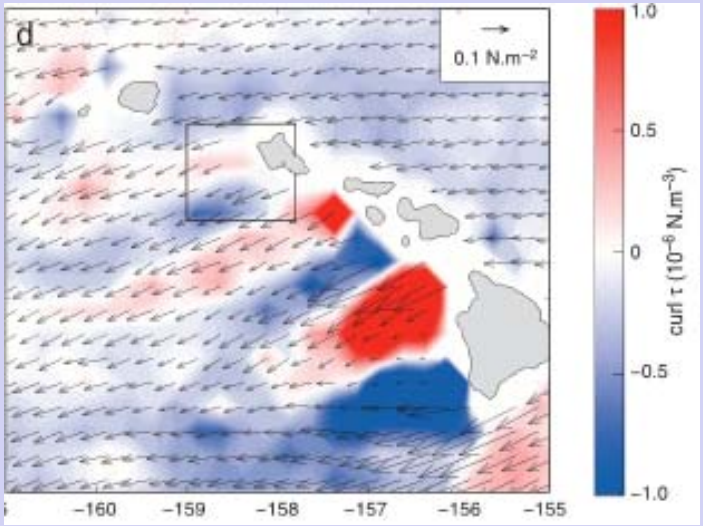

Chavanne et al. (2010)

What generates the lee eddies?

Ekman pumping or oceanic flow around the Hawaiian Islands?

Lumpkin (1998): Ekman pumping generates cyclonic eddies; flow separation at South Point of Hawaii generates anticyclonic eddies (with Ekman pumping a secondary source of downwelling).

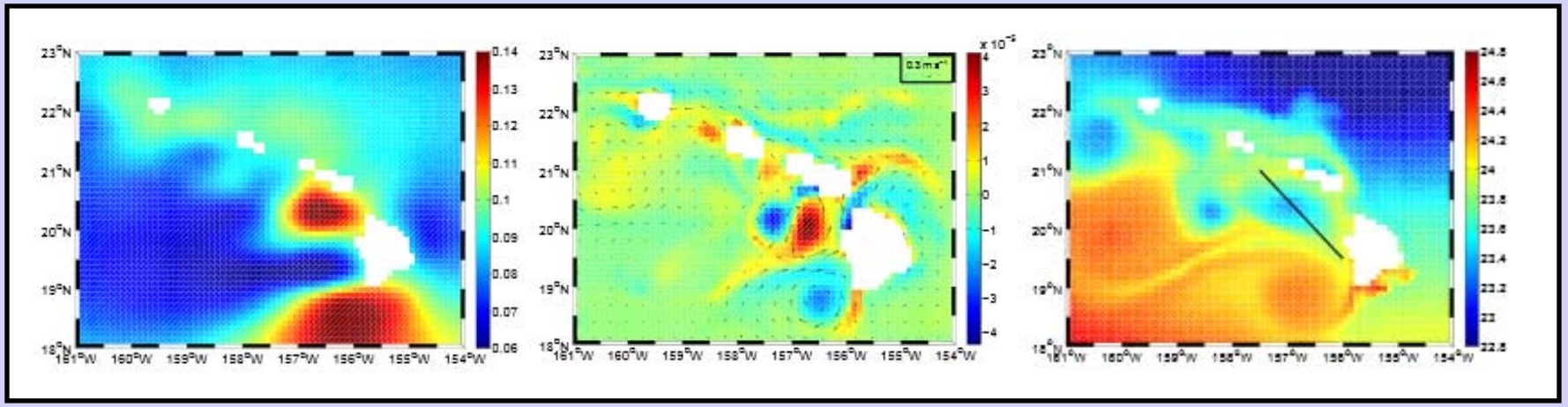

Kersalé (2011)

High-resolution simulations such as Kersalé (2011) indicate that both need to be present to generate realistically energetic eddies, along with sufficiently high resolution and forcing (QuikSCAT).

Eddies propagate westward …

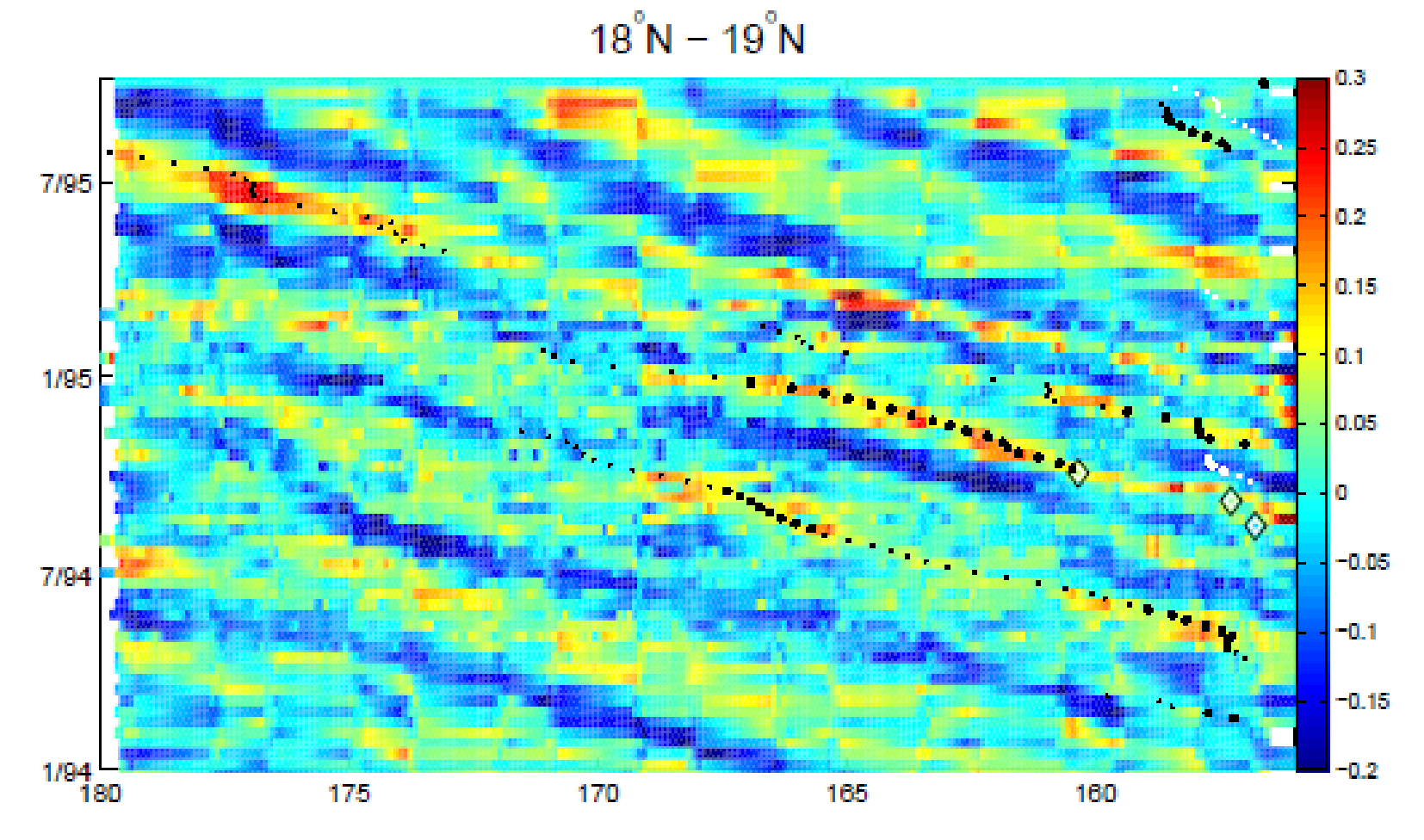

Lumpkin (1998)

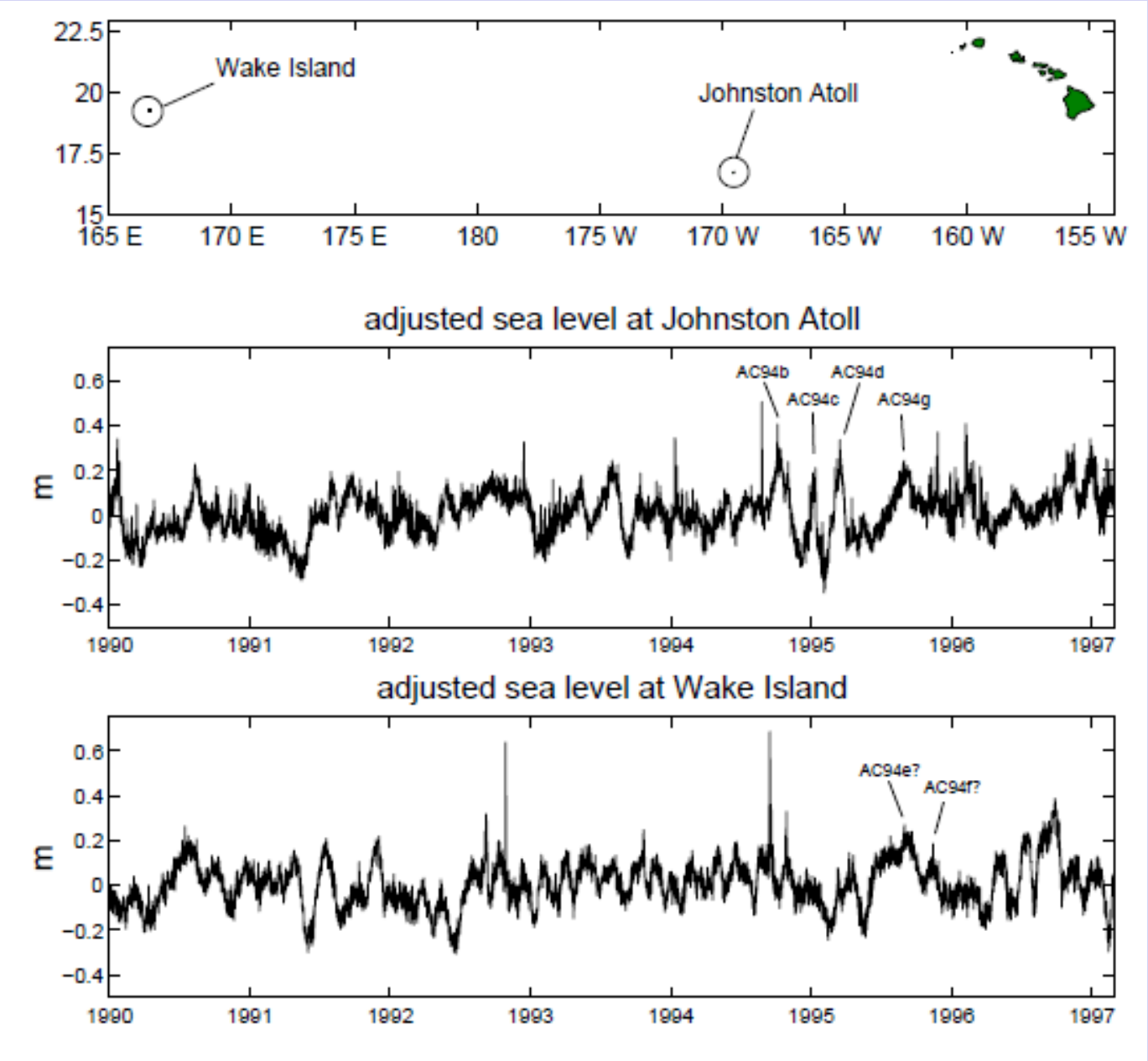

Lumpkin (1998)

Drifter observations in the HLCC

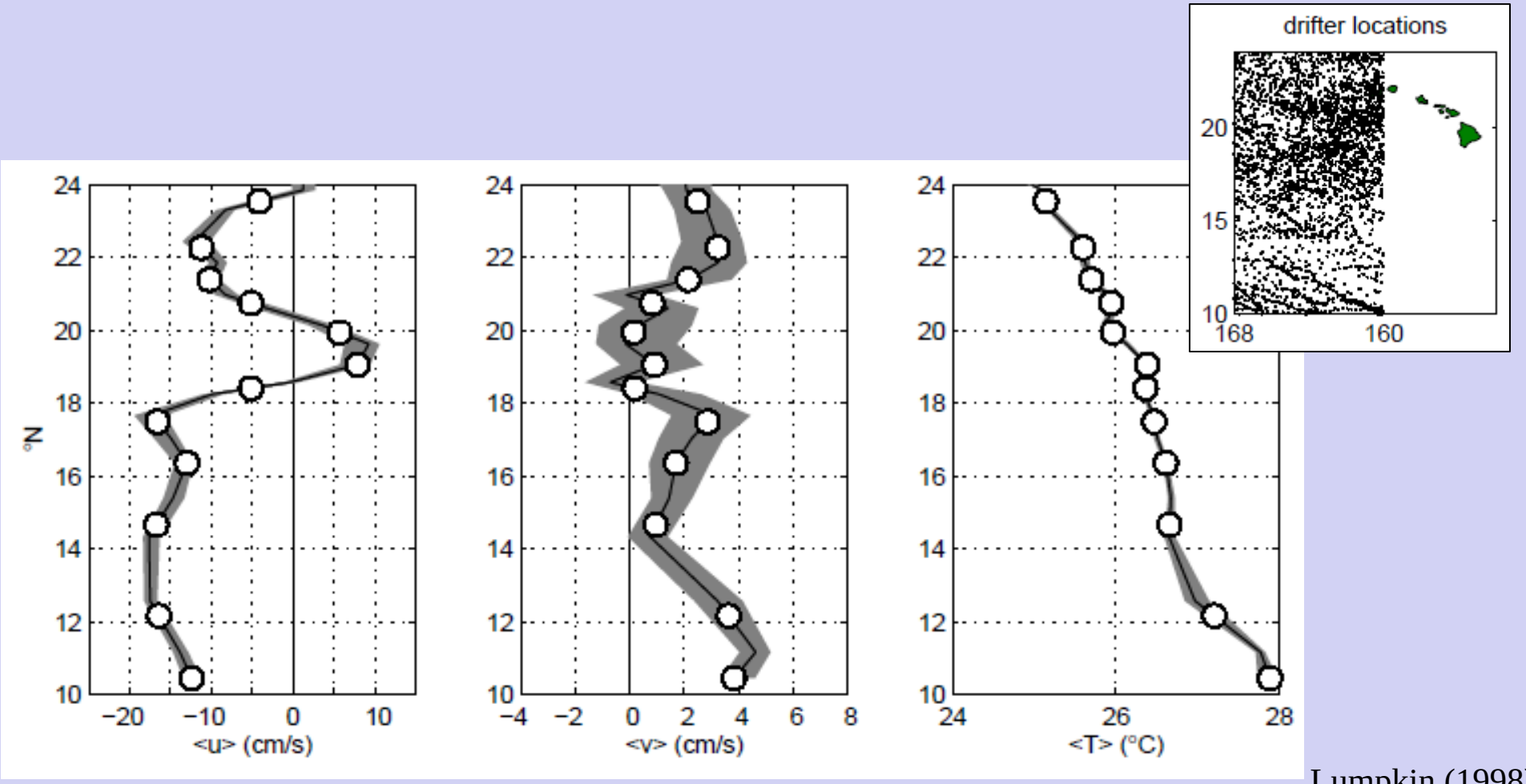

Lumpkin (1998)

Zonally averaged drogued drifter observations, 160—168°W. White circles: independent observations. Shading: standard error.

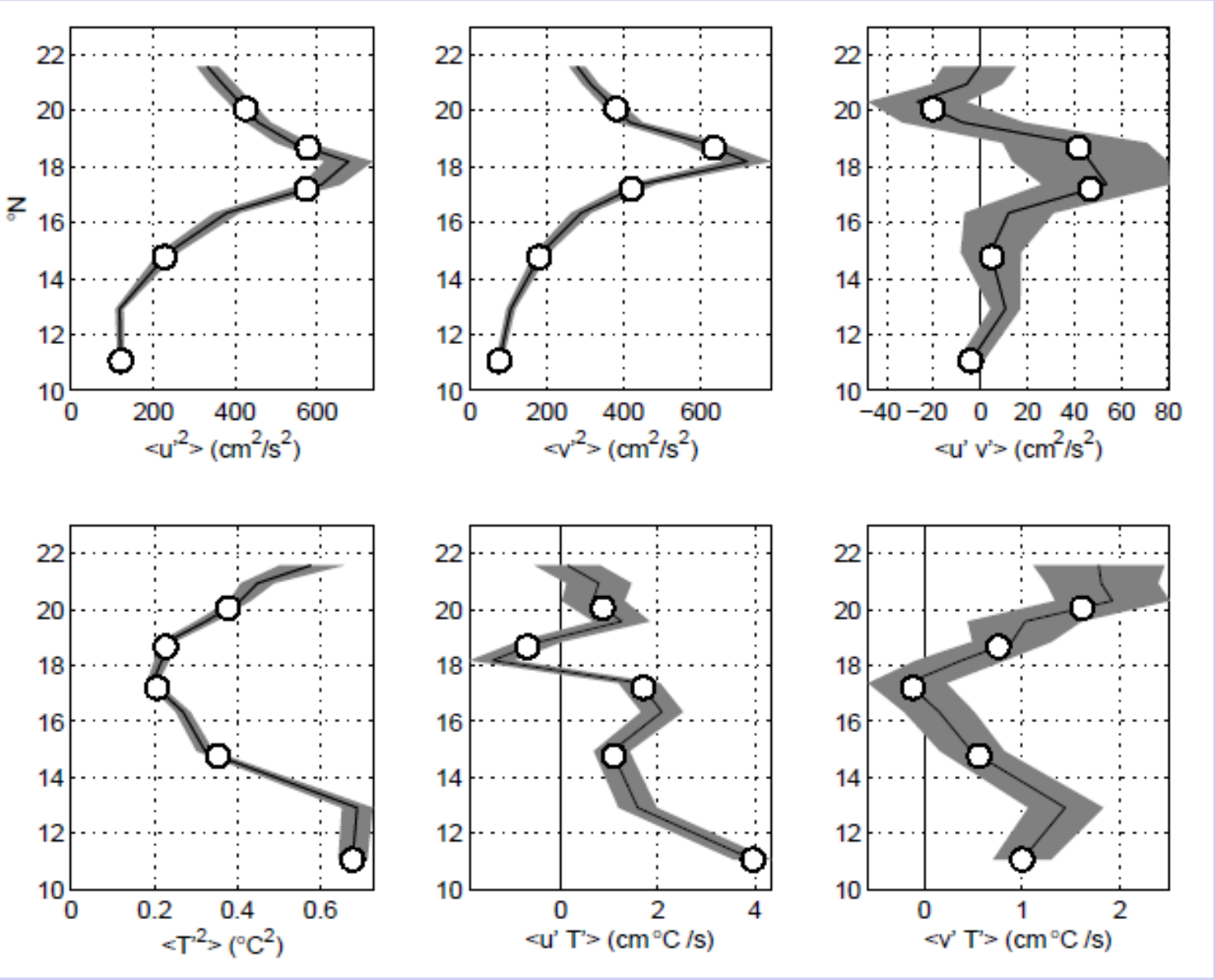

Lumpkin (1998)

Zonally averaged drifter observations, 160—168°W. White circles: independent observations. Shading: standard error.

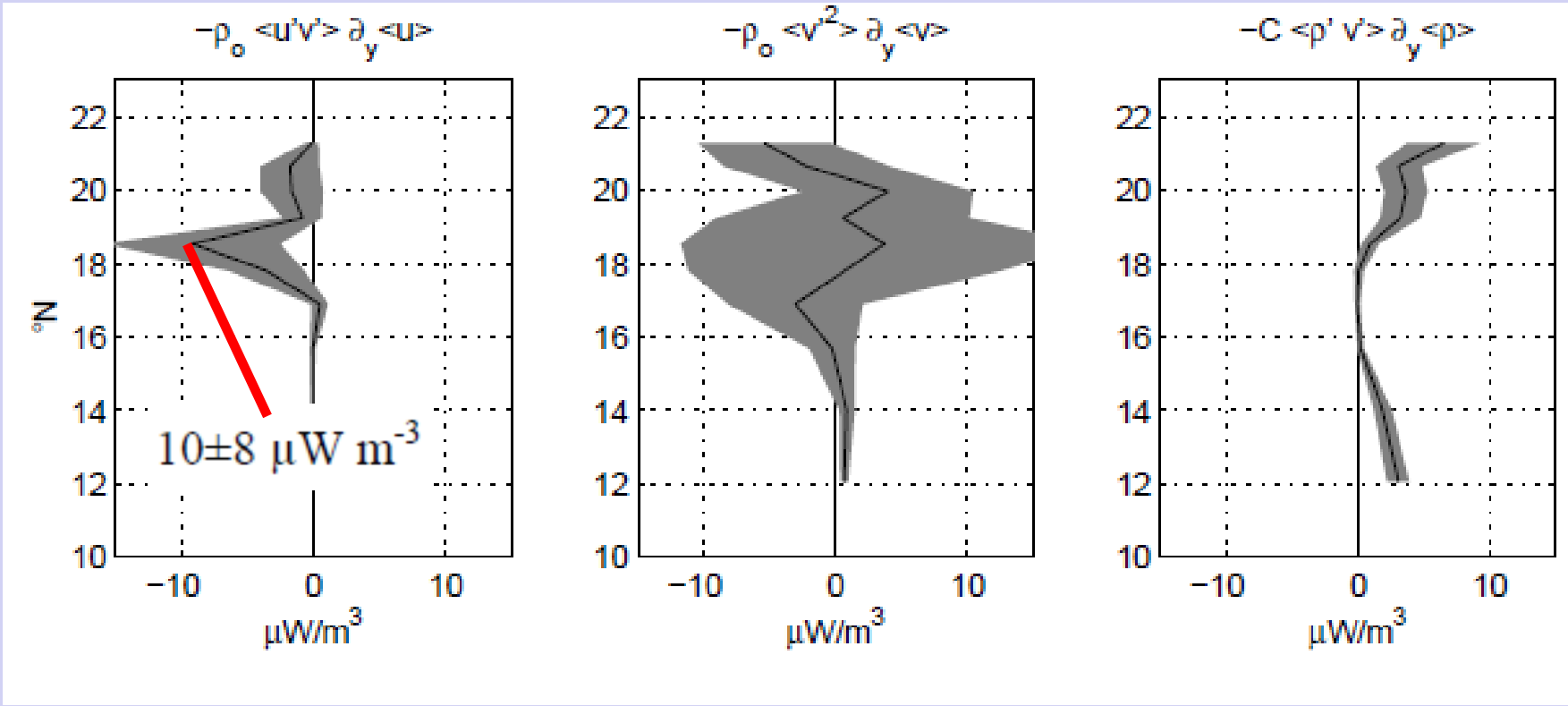

Lumpkin (1998)

Eddy fluxes from zonally averaged drifter observations, 160—168°W. Shading: standard error.

Seasonal variations of the HLCC

Wind variations

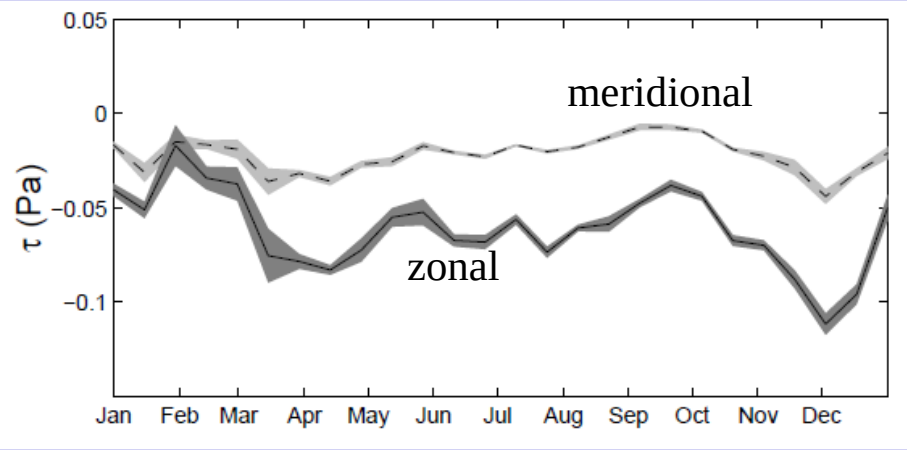

Lumpkin (1998)

HLCC variations:

Kobashi and Kawamura (2002): HLCC strongest in July to February and weakest in April to June.

Very different from STCC at ~24°N (strongest in winter through summer, weakest in fall).

What creates the HLCC?

1. Sverdrup response to large-scale wind wake (White and Walker, 1985; Leonardi, 1998; Leonardi et al., 1998; Xie et al., 2001).

2. Eddy rectification, barotropic eddy fluxes (Lumpkin, 1998; Kobashi and Kawamura (2002).

3. SST $\rightarrow$ wind feedback (Sasaki and Nonaka, 2006).

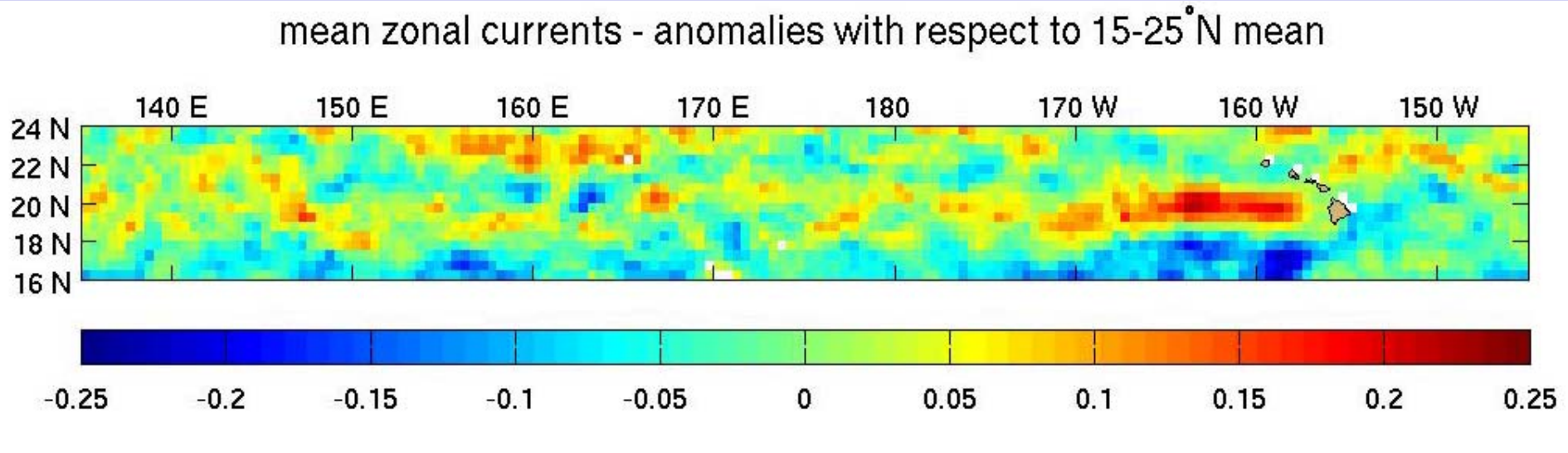
mean zonal currents - anomalies with respect to 15-25°N mean
140 E
150 E
160 E
170 E
180
170 W
160 W
150 W
24 N
22 N
20 N
18 N
16 N
-0.25
-0.2
-0.15
-0.1
-0.05
0
0.05
0.1
0.15
0.2
0.25

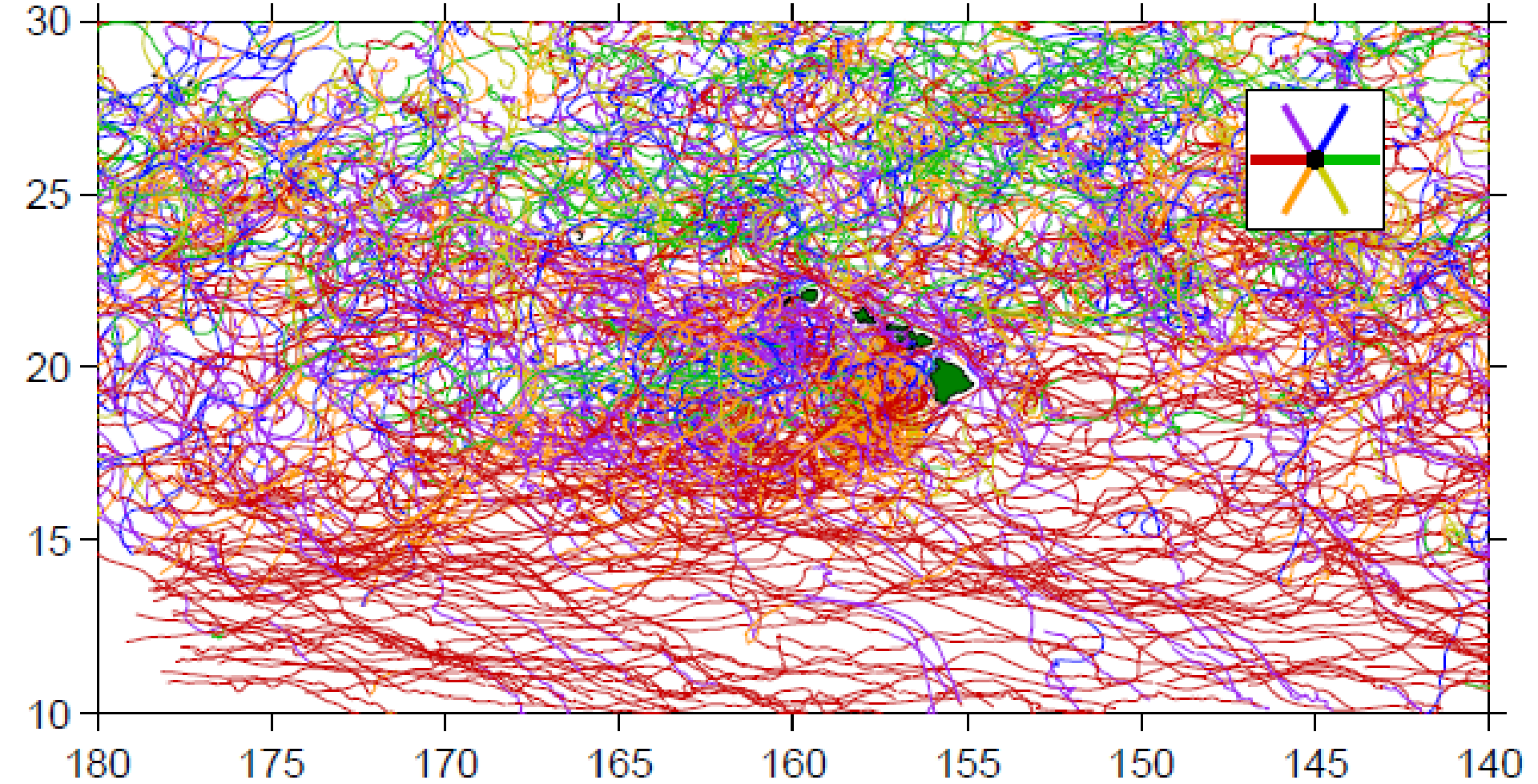

Drifter trajectories colored by direction

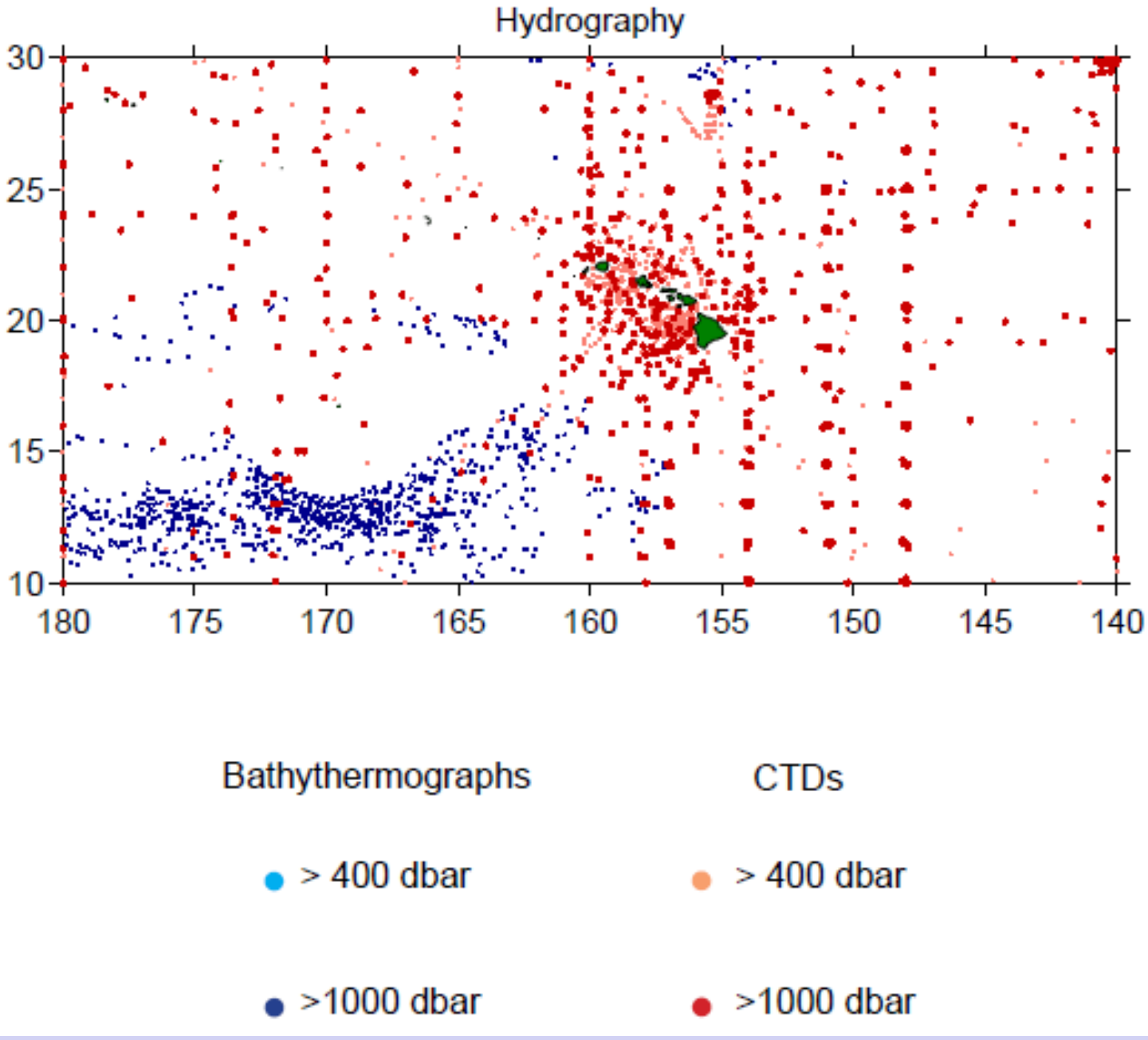
Hydrography
30
25
20
15
10
180
175
170
165
160
155
150
145
140
Bathythermographs
> 400 dbar
>1000 dbar
CTDs
> 400 dbar
>1000 dbar

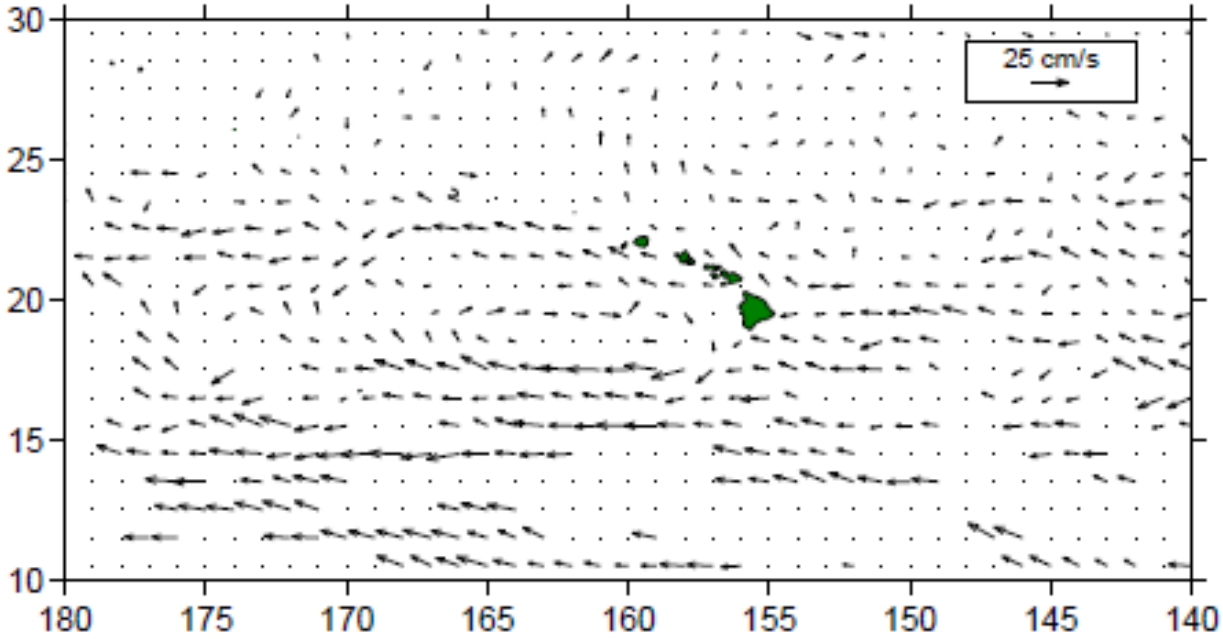

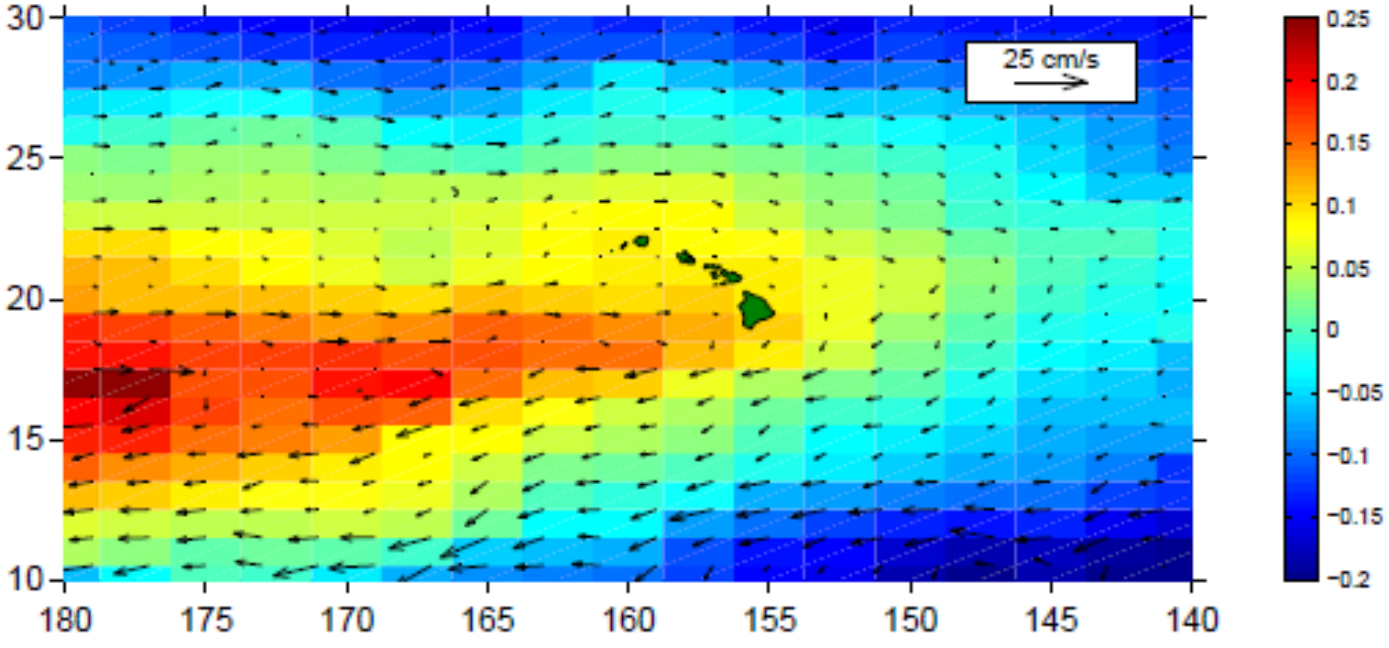

Top: mean currents from drifters.

Bottom: dynamic height anomalies relative to 400dbar from XBT, CTD (shading, m) and geostrophic currents (arrows)

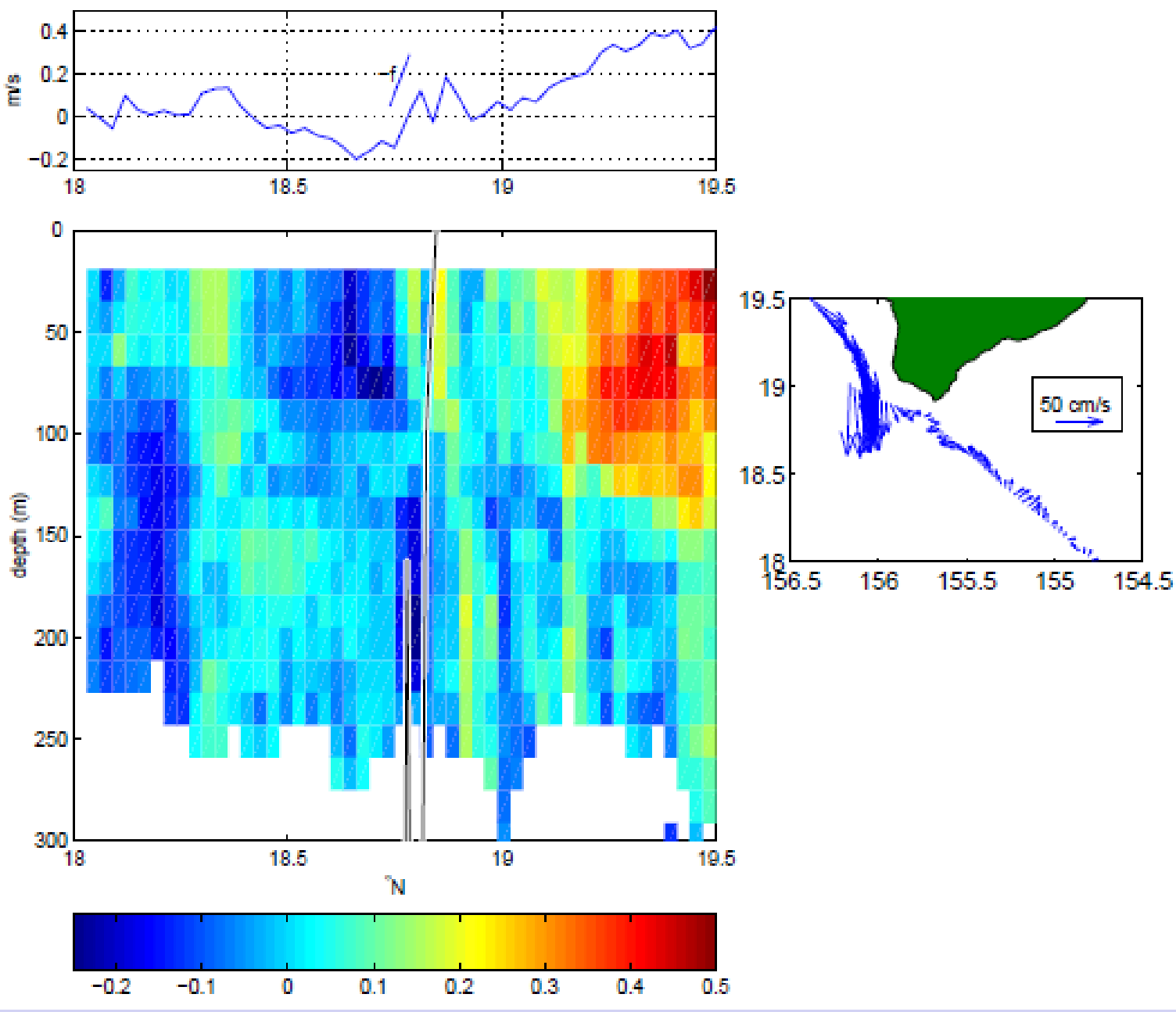
m/s
0.4
0.2
0
−0.2
−f
18
18.5
19
19.5
depth (m)
0
50
100
150
200
250
300
°N
−0.2
−0.1
0
0.1
0.2
0.3
0.4
0.5
19.5
19
18.5
18
156.5
156
155.5
155
154.5
50 cm/s